Cellular/Molecular

α_1F64 Residue at GABA$_A$ Receptor Binding Site Is Involved in Gating by Influencing the Receptor Flipping Transitions

Marcin Szczot, Magdalena Kisiel, Marta M. Czyzewska, and Jerzy W. Mozrzymas
Laboratory of Neuroscience, Department of Biophysics, Wrocław Medical University, Wrocław 50-358, Poland

GABA receptors (GABA$_A$Rs) mediate inhibition in the adult brain. These channels are heteropentamers and their ligand binding sites are localized at the $\beta(+)/\alpha(-)$ interfaces. As expected, mutations of binding-site residues affect binding kinetics but accumulating evidence indicates that gating is also altered, although the underlying mechanisms are unclear. We investigated the impact of the hydrophobic box residue localized at $\alpha_1(-)$, F64 (α_1F64), on the binding and gating of rat recombinant $\alpha_1\beta_1\gamma_2$ receptors. The analysis of current responses to rapid agonist applications confirmed a marked effect of α_1F64 mutations on agonist binding and revealed surprisingly strong effects on gating, including the disappearance of rapid desensitization, the slowing of current onset, and accelerated deactivation. Moreover, nonstationary variance analysis revealed that the α_1F64C mutation dramatically reduced the maximum open probability without altering channel conductance. Interestingly, for wild-type receptors, responses to saturating concentration of a partial agonist, P4S, showed no rapid desensitization, similar to GABA-evoked responses mediated by α_1F64C mutants. For the α_1F64L mutation, the application of the high-affinity agonist muscimol partially rescued rapid desensitization compared with responses evoked by GABA. These findings suggest that α_1F64 mutations do not disrupt desensitization mechanisms but rather affect other gating features that obscure it. Model simulations indicated that all of our observations related to α_1F64 mutations could be properly reproduced by altering the flipped state transitions that occurred after agonist binding but preceded opening. In conclusion, we propose that the α_1F64 residue may participate in linking binding and gating by influencing flipping kinetics.

Key words: **γ-aminobutyric acid; agonist binding; desensitization; GABA$_A$ receptor; receptor gating**

Introduction

GABA receptors (GABA$_A$Rs) are pentameric ligand gated ion channels that belong to the cys-loop superfamily, together with glycine receptors (GlyRs), 5-hydroxytryptamine-3 receptors (5-HT$_3$Rs), and nicotinic acetylcholine receptors (nAChRs). Ligand binding sites are localized at the $\beta(+)/\alpha(-)$ interface (Smith and Olsen, 1995; Cromer et al., 2002) and are formed by several hydrophobic residues (Padgett et al., 2007). Mutations of binding-site residues strongly affect agonist binding (Wagner et al., 2004; Goldschen-Ohm et al., 2011; Tran et al., 2011), but some effects on receptor gating have also been reported (Boileau et al., 2002; Newell et al., 2004; Venkatachalan and Czajkowski, 2008). Laha and Wagner (2011) found that disruption of a salt bridge formed by charged amino acids from the B and E loops affected binding kinetics and influenced gating, particularly desensitization. Laha and Tran (2013) reported that mutation of three conserved tyrosines at the GABA binding site profoundly affected binding and also apparently modified gating. The effects of mutations at the GABA$_A$R binding site on receptor gating may be regarded as surprising when considering the large distance between the binding site and channel gate (~5 nm) and because extensive evidence indicates that charged residues between extracellular and transmembrane domains are major determinants of cys-loop receptor gating (Kash et al., 2003; Xiu et al., 2005; for review, see Cederholm et al., 2009; Miller and Smart, 2010). The molecular mechanisms whereby the energy supplied by agonist binding is conveyed to conformational transitions remain elusive.

The hydrophobic box residue localized on $\alpha(-)$, F64 (α_1F64), has been shown to influence apparent affinity, whereas the effects on gating were only indirectly indicated (Sigel et al., 1992; Holden and Czajkowski, 2002). However, homologous (Fig. 1*A*) residues have been shown to affect gating in various cys-loop family members. Akk (2002) showed that the substitution of εW55 and δW57 to F affected the opening rate of AChRs. However, Bafna et al. (2009) suggested that the major effect of these mutations was a reduction of the binding affinity in the open state. Mutations in the homologous residue of GABA$_A$ ρ homomeric receptors (Fig. 1*A*) induced spontaneous activity (Torres and Weiss, 2002), suggesting interference with gating. Finally, a mutation of homomeric α_7 AChRs markedly slowed macroscopic desensitization (Gay et al., 2008). In previous studies (in a *Xenopus* oocyte model) concerning the α_1F64 residue, kinetic properties could

Received June 14, 2013; revised Jan. 8, 2014; accepted Jan. 14, 2014.

Author contributions: M.S. and J.W.M. designed research; M.S., M.K., and M.M.C. performed research; M.S., M.K., M.M.C., and J.W.M. analyzed data; M.S., M.K., M.M.C., and J.W.M. wrote the paper.

This work was supported by Polish National Science Centre Grant 350/B/P01/2011/40 to J.W.M. M.S. was partially supported by Wrocław Medical University Grant Pbmn80. The authors thank M. Beato for help with the ChannelLab software and M. Jatczak and W. Smigiel for technical assistance with the cell culture.

The authors declare no competing financial interests.

Correspondence should be addressed to either of the following: Marcin Szczot, Laboratory of Neuroscience, Department of Biophysics, Wrocław Medical University, ul. Chałubińskiego 3, Wrocław 50-368, Poland. E-mail: mszczot@gazeta.pl; or Jerzy W. Mozrzymas, Laboratory of Neuroscience, Department of Biophysics, Wrocław Medical University, ul. Chałubińskiego 3, Wrocław, 50-368, Poland. E-mail: jerzy.mozrzymas@umed.wroc.pl.

DOI:10.1523/JNEUROSCI.2533-13.2014

 0270-6474/14/333193-17$15.00/0

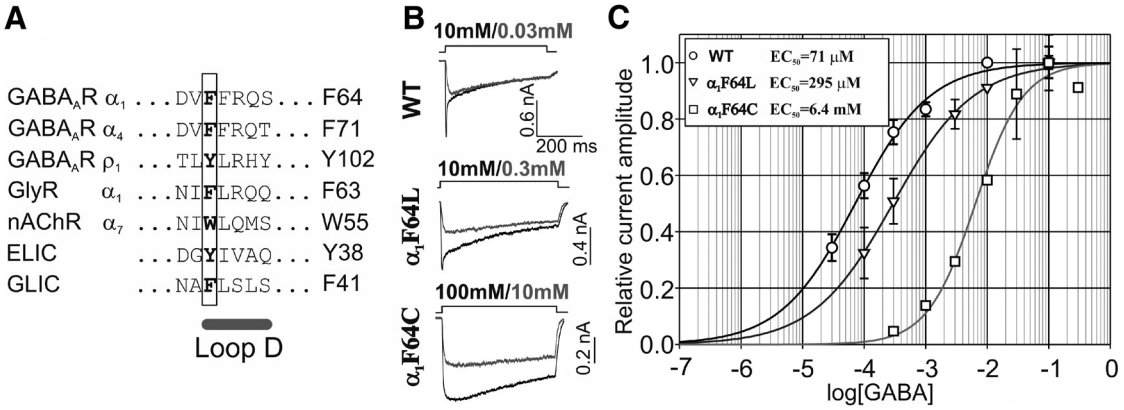

Figure 1. Mutations of α_1F64 residue right-shifted the amplitude dose–response relationships and alters the currents' kinetics. ***A***, Alignment of loop D-forming regions in different cys-loop receptors, indicating positions and numbering of residues homologous to GABA$_A$ α_1F64. ***B***, Examples of superimposed current responses to saturating (black) and nonsaturating (gray) concentrations of GABA for wild-type (WT, top), α_1F64L (middle), and α_1F64C (bottom) receptors. The insets above the current traces indicate the application time of the specified agonist concentration. ***C***, Amplitude dose–response relationships normalized to maximum currents evoked by saturating agonist and fitted by the Hill equation (Eq. 1) for WT (circles, $n_h = 0.7$), α_1F64L (triangles, $n_h = 0.7$), and α_1F64C (squares, $n_h = 1.2$).

not be fully resolved. Thus, to reliably assess the impact of α_1F64 mutations on $\alpha_1\beta_1\gamma_2$ GABA$_A$R kinetics, we used a rapid application technique. Mutations of this residue right-shifted the dose–response curves. However, they also reduced macroscopic desensitization and maximum open probability, consistent with a change in gating. Extensive experimental data based on various protocols, application of different agonists, and model simulations indicated that these effects of the α_1F64 mutation on receptor gating are mainly attributable to alterations in the flipping mechanism that precedes channel opening. We conclude that α_1F64 residue has a strong impact on both binding and gating and is likely involved in conveying the conformational transition wave down to the receptor's gate.

Materials and Methods

Cell culture, transfection, and mutagenesis. Human embryonic kidney 293 cells were cultured in DMEM (Life Technologies) supplemented with 10% fetal bovine serum (Life Technologies), 50 U/ml penicillin, and 50 U/ml streptomycin (Life Technologies), at 37°C in a 5% CO_2 incubator in Nunc flasks. Before transfection, the cells were detached from the flasks and replated in Petri dishes (BD) coated with 1 μg/ml poly-D-lysine. The cells were transiently transfected using a standard calcium phosphate precipitation method (Chen and Okayama, 1987). cDNA that encoded rat GABA$_A$R subunits cloned in pCMV vectors was mixed in the following ratio: $\alpha_1/\beta_1/\gamma_{2L}$: 1:1:3 (1:1:3 μg) in transfection solution (1 ml) together with plasmid that encoded human CD4 (1 μg). The day after transfection, the cells were detached and replated on poly-D-lysine-coated coverslips (Carl Roth). Electrophysiological experiments were performed 48–72 h after transfection. For the detection of transfected cells, CD4 magnetic binding beads were used (Dynabeads CD4, Invitrogen Dynal). The α_1F64A mutation was generated by site-directed mutagenesis method using the QuikChange mutagenesis kit (Stratagene). The coding regions of all of the plasmids were sequenced before experimental use. The plasmid that encoded the α_1F64C GABA$_A$R subunit was kindly provided by Dr. Andrea Barberis and α_1F64L was provided by Dr. Erwin Siegel.

Electrophysiological recordings. Currents were recorded in whole-cell or outside-out configurations of the patch-clamp technique at a holding potential of −40 mV using an Axopatch 200B amplifier (Molecular Devices). Signals were low-pass filtered at 10 kHz and sampled with a Digidata 1440 (Molecular Devices) acquisition card at 100 kHz and acquired with pClamp 10.2 software (Molecular Devices). Pipettes were pulled from borosilicate glass (Hilgenberg) using a PC-10 vertical puller (Narishige), and their resistance was in the 3–6 MΩ range (when filled with internal solution). For rapid agonist application, we used theta-glass capillaries driven by a piezoelectric translator (Physik Instrumente) as described in detail by Jonas (1995). Liquids were supplied to the channels of the theta-glass capillary using an SP220IZ syringe pump (WPI). The open-tip junctional potential onset (10–90% rise time) was in the 0.1–0.35 ms range. All of the current responses were elicited by a theta-glass rapid perfusion system and recorded either in the excised-patch or lifted whole-cell mode. Although currents mediated by mutants, especially cysteine mutant, were small, an effort was made to collect information on key kinetic parameters from recordings in the excised-patch configuration. Thus, all of the major kinetic features of the currents elicited by a saturating agonist (Figs. 2, 3, current traces used for simulations) were determined from recordings in the excised-patch mode. In the protocols in which analysis was based on relative values (Figs. 4–8), the highest resolution achieved in the excised patches was not critical because the lifted-cell and excised-patch data did not significantly differ and therefore were pooled.

The intrapipette solution contained the following (in mM): 137 CsCl, 1 $CaCl_2$, 2 $MgCl_2$, 11 EGTA, 2 ATP, and 10 HEPES, with the pH adjusted to 7.2 with CsOH. We used standard Ringer's solution as the external saline, which contained the following (in mM): 137 NaCl, 5 KCl, 2 $CaCl_2$, 1 $MgCl_2$, 20 glucose, and 10 HEPES, with the pH adjusted to 7.2 with NaOH. To avoid osmolarity artifacts for agonist concentrations >10 mM, the extracellular NaCl concentration was reduced to 87 mM, and the wash solution was adjusted with glucose to maintain constant osmolarity. To ensure unchanged chloride reversal potential, the CsCl concentration in the intrapipette solution was also reduced to 87 mM and supplemented with 50 mM K-gluconate (Wagner et al., 2004; Goldschen-Ohm et al., 2011). Test measurements confirmed that none of these modifications affected the kinetics or amplitude of the measured currents. Access resistance was monitored (typical value, 5–10 MΩ) and compensation was routinely applied to currents that exceeded 2 nA. However, current responses that were characterized by such a large peak amplitude were excluded from quantitative kinetic fitting and only used for comparisons of current amplitudes between GABA-evoked and pentobarbital (PB)-evoked currents in wild-type and mutant receptors. Test recordings (i.e., comparison of currents measured with and without compensations) showed that below this current value (2 nA), the compensation effect was negligible. Cells with excessive or unstable access resistance were excluded from the analysis. The instability of recorded signals (rundown or runup) was assessed by repeating the current recordings ≥3 times and alternating the test recordings elicited, for example, by muscimol and PB with control sweeps evoked by GABA and corrected using the linear interpolation method. Records that showed excessive drift that exceeded 20% during the recording period were excluded from the analysis. All of the chemicals were purchased from

Sigma-Aldrich. All of the experiments were performed at room temperature (22–24°C).

Chloride depletion does not affect fast kinetics of GABAergic currents. Recent work by Karlsson et al., 2011 raised the possibility that the time course of current responses might be influenced by the depletion of chloride ions. Thus, assessing the impact of this phenomenon on our recordings was important. Currents recorded in excised patches did not show any detectable dependence between the extent of desensitization and current amplitude (data not shown). Moreover, in both recording configurations, the application of a saturating agonist pulse at 0 mV (i.e., no chloride depletion due to negligible driving force), followed by a voltage step to −40 mV (while the agonist was continuously present) resulted in the current practically overlapping (starting from the moment of voltage jump to −40 mV) with responses elicited by the same agonist application at a constant membrane voltage of −40 mV (data not shown). This observation proves that current fading was attributable to a conductance change rather than chloride depletion. To additionally assess the impact of chloride depletion in the excised-patch mode, we applied simulations employed previously by Moroni et al. (2011). We chose parameters that favored chloride depletion to a larger extent than expected under our experimental conditions (50 nS conductance, which is twice the largest conductance measured here; 1.1 μm small excised patch radius; thick and long membrane section that clogged the lumen of the pipette; $p = 2$ μM; $f = 0.2$). Assuming a nondesensitizing current, simulated chloride depletion elicited a ~15% current reduction 10 ms after the peak, and the time constant of fading was nearly one order of magnitude slower than the one observed in our experiments (i.e., ~25 ms for chloride depletion vs 2 ms in our excised-patch recordings). In addition, considering in this model a desensitizing conductance, we found that chloride depletion did not affect the current fading kinetics for desensitization time constants <30 ms (data not shown). Considering these data and estimations, we are confident that the impact of chloride depletion on our recordings was negligible because this phenomenon becomes significant for responses evoked by agonist applications that are much longer and larger (Karlsson et al., 2011) than those considered in the present work.

Data analysis. The recorded current traces were analyzed using pClamp 10.2 software (Molecular Devices). Normalized dose–response relationships were fitted using Equation 1, the Hill equation:

$$EC = \frac{1}{1 + \left(\frac{EC_{50}}{[GABA]}\right)^{n_h}}$$

EC_{50} is half-maximal concentration, and n_h is the Hill coefficient. The current onset was assessed as 10–90% rise time (t_{Rise}). For noisy traces, the rise time was assessed by exponential fitting as shown in the following Equation 2:

$$I(t) = A \cdot \left(1 - \exp\left(-\frac{t}{\tau}\right)\right)$$

A is the current amplitude, and τ is the time constant. The 10–90% rise time was then calculated using the following formula, Equation 3:

$$t_{Rise} = \tau \cdot ln9$$

The deactivation of currents for various agonists was fitted using exponential functions, in which one or two components were typically sufficient, as shown in the following Equation 4:

$$I(t) = \sum_{n=1}^{f} A_n \cdot \exp\left(-\frac{t}{\tau_n}\right)$$

A_n is the respective amplitude component and τ_n is the time constant. The mean time constant was calculated using the following formula, Equation 5:

$$\tau_{mean} = \sum_{n=1}^{f} a_n \tau_n$$

a_n is the normalized weight of the respective components calculated as $a_n = A_n / \Sigma_k A_k$. The rapid component of desensitization onset induced by prolonged agonist application at saturating concentrations was described by fitting the following exponential function, Equation 6:

$$I(t) = A \cdot \exp\left(-\frac{t}{\tau_{des}}\right) + C$$

A is the amplitude of the desensitizing component. τ_{des} is the time constant. C is the constant value. In the case of rapidly desensitizing receptors, the time constant values were typically between 1.5 and 6 ms; therefore, the fit was usually performed for the time window of ~10 ms, starting from the peak. For some mutants, desensitization onset was slow, and fitting the exponentials was problematic. In such cases, the extent of desensitization was quantified as the relative current reduction 10 ms after the peak: $FR(10) = \frac{I_{t=10ms}}{I_{max}}$. I_{max} is the maximum current value, and $I_{t=10ms}$ is the value of the current at $t = 10$ ms after the peak. The statistical analyses were performed using SigmaPlot 11.0 software (SPSS) and Excel 2010 (Microsoft). The normality of the data distributions was checked using the Shapiro–Wilk test. Comparisons between groups with distributions classified as normal were made using Student's t test, with the confidence interval set at level 0.05. Data characterized by non-normal distributions were analyzed using the nonparametric Mann–Whitney test and confidence interval was set at the same level. The data are expressed as mean ± SEM. To estimate the error of the parameters that depended on one or more experimentally measured coefficients (e.g., determination of k_{on} using the race method), combined standard uncertainty was calculated. Briefly, the uncertainty of the calculated parameter, described as a function of measured values, may be calculated as a sum of the given function partial derivatives with respect to the variables (i.e., measured values) multiplied by the measured value uncertainty according to the following equation:

$$\Delta F = \sum_{i=1}^{n} \left| \frac{\partial F(p_1, p_2, \ldots, p_n)}{\partial p_i} \Delta p_i \right|$$

ΔF is the calculated uncertainty value. $F(p_1, p_2, \ldots p_n)$ is the function of measured values that describe the parameter. Δp_i is the uncertainty of the measured parameter.

Nonstationary variance analysis. Nonstationary variance analysis (Sigworth, 1980) was performed as described previously (Wagner et al., 2004). Briefly, ≥10 consecutive responses to saturating agonist concentrations were recorded from the same patch. The currents were analyzed using custom MatLab program (Mathworks). For each time point, the mean current (I) and variance (σ^2) were calculated. The values of mean current were then divided into 100 equal bins and the mean variance was calculated for variances associated with the mean current values included in the specific bin. Variance was plotted versus the mean current and fitted with the equation: $\sigma^2 = iI - I^2N^{-1} + c$, where i is the single-channel current, N is the number of channels, and c is the baseline noise variance (Ghavanini et al., 2006). The maximum open probability was calculated as the maximum current divided by $i \cdot N$. Single-channel conductance was calculated by dividing the single-channel current i by the electrical driving force (−40 mV), which is represented by the holding voltage in symmetrical chloride. Current onset was excluded from the analysis because even minimal jitter in the current rising phases resulted in a substantial overestimation of variance biasing. Thus the estimation of the respective parameters (De Koninck and Mody, 1994) and starting point for the analysis were set at the peak of the response.

Measurement of competitive antagonist microscopic binding rates. To measure competitive antagonist [gabazine (GBZ) in our experiments] binding and unbinding rates, we adopted protocols described in detail in previous studies (Jones et al., 1998, 2001). To determine the microscopic binding and unbinding rates for GBZ, patches were pre-equilibrated in the presence of GBZ, and a saturating concentration of GABA was subsequently applied. The time course of the resulting current response reflected a convolution of antagonist unbinding and agonist-induced activation kinetics. Control current responses (i.e., with no pre-equilibration with the antagonist) were recorded each time from the

same patch before and after recordings with GBZ pretreatment, allowing the additional assessment of current rundown. Numerical deconvolution yielded an unbinding time course for GBZ ($k_{off\text{-}GBZ}$) and the percentage of receptors occupied by the antagonist at equilibrium. A fast Fourier transform (FFT)-based custom MatLab program (Mathworks) was used to perform the deconvolution procedure in a 300–500 ms window. To reduce FFT artifacts in time-limited signals, signal ends were supplemented with zeros, and the entire signal was multiplied by a sigmoid window function before deconvolution (Jones et al., 2001). Repeating this protocol for a range of the antagonist concentrations allowed us to construct the relationship between initial receptor availability and antagonist concentration. At low antagonist concentrations at which the deconvolution trace was flat, the initial availability was assumed to be 1. The relationship between receptor availability and antagonist concentration was fitted with the Hill equation (assuming Hill coefficient equals 1; Jones et al., 2001) and the equilibrium constant (half-blocking concentration) for antagonist binding (KD-GBZ) was determined. The antagonist binding rate was determined as $k_{on-GBZ} = \frac{k_{off-GBZ}}{KD - GBZ}$ (Jones et al., 2001).

Estimation of microscopic GABA binding rate. The microscopic GABA binding rate was determined using the "race" protocol (Jones et al., 1998). Thus, saturating [GABA] was coapplied with subsaturating [GBZ]. For given GABA and GBZ concentrations, the amplitude of such a response normalized to the amplitude of the control current elicited by GABA alone (termed I_{race}) depends only on the ratio of the agonist and antagonist binding rates. Thus, the agonist binding rate can be estimated from the following Equation 7:

$$k_{on} = \frac{[GBZ] \cdot k_{on\text{-}GBZ}}{2 \cdot [GABA] \cdot \left(\frac{1}{I_{race}} - 1\right)}$$

This equation assumes that GBZ binds to only one site on the receptor, and binding at that site prevents binding of the GABA molecule (Wagner et al., 2004; Jones et al., 1998). Although the deconvolution protocol assumes purely competitive action of an antagonist, some data (Ueno et al., 1997) suggest that GBZ may allosterically affect the receptor. However, as suggested by Jones et al. (1998) and Goldschen-Ohm et al. (2011), such an action would not significantly distort the estimation of the parameters extracted using the deconvolution procedure. Notably, the reliable estimation of k_{on} using the race experiment requires that the receptor must bind antagonist or agonist only once before the current peak (Wagner et al., 2004). This is fulfilled for wild-type receptors for which GBZ unbinding is slow and activation is fast. However, in the case of mutant receptors, GBZ unbinding is relatively fast, and the subsequent binding of GABA before the current peak cannot be excluded. Still, considering that GBZ $\tau_{off\text{-}GBZ}$ is ~20 ms, and the time-to-peak is close to 1 ms, only ~5% of the receptors would be expected to unbind GBZ before the current reaches its maximum value, and only fraction of these would bind GABA and open before the current reaches its peak, indicating that this effect would have a negligible impact on the estimation of the k_{on} rate constant. In our experiments, GBZ was used at a concentration that inhibited nearly 50% of the measured current.

Kinetic modeling. Model simulations were performed, using ChannelLab 2.0 software (Synaptosoft), for four different minimum requirement schemes that were either previously used for kinetic modeling of $GABA_A$Rs [Fig. 9*A*, Jones–Westbrook Model (JWM) and Linear Model (LM)] or offered additional insights into the activation mechanism [Fig. 10*A*, flipped Jones–Westbrook Model (fJWM) and flipped Linear Model (fLM)]. To optimize the rate constants in the considered models, a waveform-fitting module was used, and the responses to long and short pulses of saturating GABA concentrations (modeled as a square application wave) were numerically fitted. Because recordings from lifted cells (whole cell) were characterized by a relatively slow solution exchange, only current responses recorded from excised patches were used for the model simulations. Fits were performed for responses collected from each patch separately, thus yielding one complete set of the rate constants for each patch. The final estimation of the rate constants for each considered model was based on the statistics of the respective parameters established for all of the patches included in the analysis. During the optimization procedure, k_{on} was set to a value established in the racing protocol unless otherwise specified (see Results). To fit currents mediated by wild-type receptors, rate constants that shaped the onset phase (d, β, γ) were optimized for a short time interval, including the current rising phase, whereas other rate constants were constrained to parameter values for $GABA_A$Rs taken from Mozrzymas et al. (2003b). Therefore, the obtained values of d, β, and γ were used as optimal estimations in the second step, in which the remaining rate constants were unconstrained, and the traces were fitted over the entire considered time course (typically ≤500 ms for short-pulse applications and 15–30 ms for long-pulse applications).

The fitting of responses mediated by the α_1F64C mutants began with constrained desensitization (d, r) or efficacy (β, α) and unbinding (k_{off}) rate constants at values determined for wild-type receptors. Subsequently, desensitization and efficacy were unconstrained. In the mutants, the unbinding rate had to be constrained at the value determined for wild-type receptors because otherwise the optimization algorithm tended to increase k_{off} to values that rendered the simulated responses very distant from saturation, contrary to the experiment.

The effects of α_1F64L mutation were considered for responses evoked by saturating agonists (GABA and muscimol); therefore, only rate constants that governed gating were assessed. For this purpose, in the respective models, flip rate constants were manually varied to best reproduce the kinetic trends of the recorded currents. Manually adjusted or constrained rate constants are presented in tables without SE values. The relationships between the major kinetic features of simulated responses and respective rate constants are presented either in the form of curve families, which are obtained by simulating current responses by varying a specific rate constant (Fig. 9), or in the form of surface plots (Fig. 10). The latter were applied to illustrate trends between the respective kinetic parameters of simulated responses and the two rate constants that governed flipping transitions (Fig. 10). Surface plot data were generated using custom Autohotkey scripts (developed by Chris Mallett and Steve Gray, GNU General Public License) to perform automated multiple Monte Carlo simulations for at least 20,000 channels for a range of tested rate constants in ChannelLab software. To avoid the excessive impact of stochastic noise in the Monte Carlo simulations, some surface plots, especially for conditions of low open probability, represent averages of 5–10 simulation runs.

Results

Mutations of the α_1F64 residue strongly affect the apparent affinity and kinetics of currents mediated by $\alpha_1\beta_1\gamma_2$ receptors

In the oocyte expression system in previous studies, both the α_1F64L (Sigel et al., 1992) and α_1F64C (Holden and Czajkowski, 2002) mutations induced a strong rightward shift in the dose–response relationships, suggesting dramatic interference with receptor binding properties. To determine whether changes in binding characteristics are accompanied by gating alterations, we measured high-resolution current responses to rapid GABA applications for wild-type and mutant (α_1F64L and α_1F64C) receptors over a wide range of agonist concentrations. As expected, these mutations markedly right-shifted the dose–response curves (Fig. 1*B*,*C*). Notably, whereas the α_1F64L mutation caused an ~4-fold increase in EC_{50}, a >100-fold increase was observed for α_1F64C mutants. Basing on these dose–response relationships, we chose the following saturating GABA concentrations for specific mutant and wild-type receptors: wild type, 10 mM; α_1F64L, 100 mM; α_1F64C, 100 mM. The durations of the agonist application times were chosen to either include the entire rising phase and the peak or detect the plateau values (Fig. 2).

Although ascribing changes in the EC_{50} values or Hill coefficient to the modulation of binding characteristics is tempting, the modulation of receptor gating might also affect both of these parameters (Colquhoun, 1998; Mozrzymas et al., 2003a; Wagner

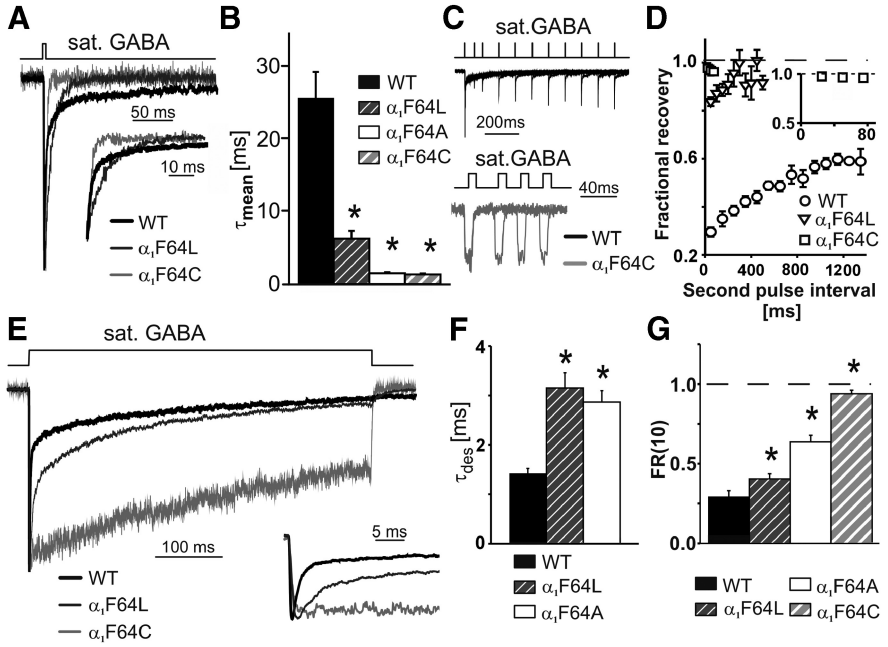

Figure 2. Mutation of α_1F64 residue strongly accelerates deactivation and slows down macroscopic desensitization in current responses evoked by saturating GABA concentrations. ***A***, Superimposed and normalized traces of responses to short pulses of saturating GABA concentration for wild-type (WT) and mutated receptors. In the inset, the same traces are shown in the expanded time scale. A saturating [GABA] concentration was chosen based on dose–response data: WT, 10 mM; α_1F64L, 100 mM; α_1F64C, 100 mM. Because the alanine mutant produced weaker alterations in current responses than the cysteine mutant, we assumed 100 mM as saturating concentration for α_1F64A receptors. Because the onset kinetics of currents mediated by the mutant receptors was slower than in WT receptors, the durations of agonist application were chosen to include the entire rising phase and peak or maximum values: WT, 1–3 ms; α_1F64L, 1–3 ms; α_1F64A, 1–3 ms; α_1F64C, 2–5 ms. ***B***, Summary of mean deactivation time constants (τ_{mean}) determined for WT and mutated receptors. Notice that with respect to ***A***, additional data for α_1F64A mutants are presented. ***C***, Comparison of current responses evoked by the paired-pulse protocol with an increasing interpulse interval for WT (top, black traces) and α_1F64C (bottom, gray traces) receptors. Notice that for currents mediated by WT receptors, recovery after the first pulse was gradual because of accumulation in desensitized states, but in the case of α_1F64C mutants, the amplitudes of the currents elicited by the first and second pulses were indistinguishable, regardless of the interpulse duration. ***D***, Statistics of the extent of recovery for currents elicited by the second pulse versus interpulse interval for WT and mutated receptors. In the inset, recovery for the α_1F64C mutants is shown in the expanded time scale. ***E***, Superimposed and normalized traces of responses to long (500 ms) pulses of saturating [GABA] for WT and mutated receptors. In the inset, the same traces are shown in the expanded time scale. Notice the lack of a fast macroscopic desensitization component in the case of α_1F64C receptors. Because α_1F64L and α_1F64A mutants showed similar desensitization kinetics, the current trace for F64A is not presented in ***E*** for clarity. ***F***, Statistics for the fast desensitization time constant (τ_{des}) for WT and mutated receptors (see Results for numerical values). Notice that the value of τ_{des} for the cysteine mutant is not presented in this chart because an exponential fit was unavailable for this trace (***E***, inset). ***G***, Comparison of current remaining after 10 ms after the peak [FR(10)]. See Results for numerical values. The insets above the current traces indicate the application time of the specified agonist. Asterisks indicate a statistically significant difference. All of the data were acquired in the excised patch configuration.

et al., 2004). Notably, as shown in Figure 1*B*, the sample current traces for wild-type receptors and the respective mutant receptors showed profoundly different time courses, indicating that the mutations might indeed be associated with substantial alterations in receptor gating. To specifically address the impact of the mutations on receptor gating properties, we compared the macroscopic kinetics of currents mediated by wild-type and mutant receptors. Importantly, however, a precise estimation of how a considered mutation affects a specific gating property is difficult because any kinetic feature of the recorded currents (e.g., rise time, macroscopic desensitization, or deactivation) may potentially depend on all of the rate constants in the considered gating scheme (Colquhoun and Hawkes, 1982, 1995; Colquhoun, 1998; Mozrzymas et al., 2003a). Thus, to reduce the number of degrees of freedom in modeling the current responses, we employed numerous agonist application protocols and used different agonists. This extensive body of experimental data was subsequently used in the simulations (see Model simulations and Discussion) to indicate the mechanisms by which the considered mutations affect receptor function.

We first investigated the deactivation kinetics for currents elicited by short and saturating GABA pulses (Fig. 2*A*,*B*), which are believed to strongly depend on unbinding and desensitization (Bianchi et al., 2007). We found that all of the α_1F64 mutant receptors, compared with wild-type receptors, exhibited a dramatically faster deactivation time course (τ_{mean}: wild type, 25.9 ± 3.6 ms, $n = 11$; α_1F64L, 6.3 ± 1.1 ms, $n = 9$, $p = 2.77 \cdot 10^{-4}$; α_1F64A, 1.3 ± 0.1 ms, $n = 7$, $p = 4.96 \cdot 10^{-5}$; α_1F64C, 1.5 ± 0.2 ms, $n = 11$, $p = 5.38 \cdot 10^{-5}$; Fig. 2*A*,*B*). Importantly, whereas the deactivation kinetics in wild-type receptors were clearly biphasic (τ_{fast}, 4.2 ± 1.2 ms; τ_{slow}, 122.9 ± 17.8 ms; A_{fast}, 0.74 ± 0.03; A_{slow}, 0.26 ± 0.03; $n = 11$), only one exponential function was needed to describe deactivation for all of the considered mutants.

In the protocol in which a pair of short pulses of saturating [GABA] were applied, consistent with previous reports (Mozrzymas et al., 2003a; Wagner et al., 2004), we observed that the amplitude of the second response for wild-type receptors was markedly smaller than the first one (Fig. 2*C*) revealing an accumulation of receptors in the desensitized state(s). Interestingly, as shown in Figure 2*D*, for the leucine mutant, the reduction of the second pulse was dramatically reduced with respect to the wild type, whereas for the cysteine mutant no such reduction was observed at any interpulse interval. To further explore the effects of the mutations on macroscopic desensitization, we applied a standard protocol of prolonged 500 ms application of saturating agonist. Unexpectedly, we found that α_1F64 mutations had a strong effect on the rapid component of current fading attributable to desensitization onset, and the α_1F64C mutation practically abolished it (Fig. 2*E*–*G*). For wild-type receptors and the α_1F64L and α_1F64A mutant receptors, the fast desensitization time constants could be determined by fitting the time course with the exponential function (Fig. 2*F*). For very weakly desensitizing α_1F64C receptors, this process was assessed as a fraction of the current that remained 10 ms after the peak [FR(10); see Materials and Methods; Fig. 2*G*; for the sake of comparison FR(10) was also determined for other receptors]. As shown in Figure 2*F*, the mutations significantly prolonged τ_{des} (wild type: 1.4 ± 0.1 ms, $n = 11$; α_1F64L: 3.2 ± 0.3 ms, $n = 12$; $p = 1.15 \cdot 10^{-4}$; α_1F64A: 2.9 ± 0.2 ms, $n = 7$; $p = 0.023$). Weakening of the extent of desensitization was well illustrated by a marked increase in the FR(10) (wild type: 0.29 ± 0.04, $n = 11$; α_1F64A: 0.63 ± 0.04, $n = 7$, $p = 1.87 \cdot 10^{-5}$; α_1F64L: 0.40 ± 0.03, $n = 12$, $p = 0.03$; α_1F64C: 0.93 ± 0.02, $n = 14$, $p = 1.03 \cdot 10^{-13}$, the p values were determined for comparison with

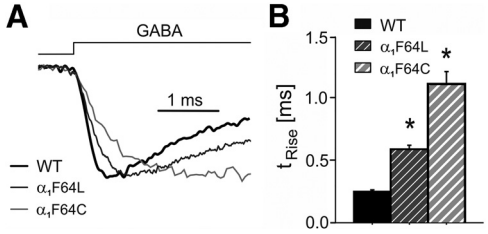

Figure 3. Onset kinetics of currents evoked by saturating GABA concentration are slowed by mutation of α_1F64 residue. ***A***, Examples of normalized and superimposed currents mediated by wild-type (WT), α_1F64C, and α_1F64L receptors. Statistics for 10–90% rise time measured for responses mediated by the considered receptors are shown (GABA concentrations: 10 mM for WT; 100 mM for α_1F64L and α_1F64C). Notice that the mutations, especially α_1F64C, slowed the current onset rate. The insets above the current traces indicate the application time. ***B***, Statistics for the t_{Rise} durations for WT and mutated receptors (see Results for numerical values). Asterisks indicate a statistically significant difference.

wild-type receptors). Overall, these results provide evidence that mutations of the α_1F64 residue not only affected agonist binding but also strongly influenced receptor gating. In particular, these mutations appeared to disrupt rapid desensitization, although our subsequent experiments and analysis suggested an alternative possibility (see Model Simulations, Discussion).

α_1F64 mutations affect current onset

The onset of the current response to nonsaturating agonist application depends on both binding and gating, whereas for saturating doses, it is believed to critically depend on receptor gating (e.g., Maconochie et al., 1994; Mozrzymas et al., 2003a,b). Thus, we determined how mutations of the α_1F64 residue affects this parameter in the considered receptors. We compared the onset kinetics of currents mediated by wild-type and α_1F64 mutant receptors. Importantly, because the current rise time kinetics, especially when elicited by saturating agonist application, may show submillisecond kinetics (Mozrzymas et al., 2003a), its reliable determination critically depends on the effective speed of solution exchange. Thus, recordings of this parameter were made exclusively in the excised-patch configuration. As expected, using as a basis our previous experiments with neurons and recombinant GABA$_A$Rs (Mozrzymas et al., 2003b), the 10–90% t_{Rise} for currents mediated by wild-type receptors, at a saturating [GABA], was very fast (0.25 ± 0.01 ms, $n = 12$; Fig. 3*A*,*B*) and it was modestly prolonged in α_1F64L mutants (0.60 ± 0.04 ms, $n = 16$, $p = 7.90 \cdot 10^{-4}$; Fig. 3*A*,*B*). In the case of α_1F64C mutants, the 10–90% t_{Rise} for currents mediated by wild-type receptors was strongly slowed (t_{Rise}: 1.12 ± 0.11 ms, $n = 9$, $p = 3.17 \cdot 10^{-5}$, compared with wild type; unpaired t test; Fig. 3*A*,*B*), further indicating the impact of α_1F64 mutations on gating.

α_1F64C mutation decreases microscopic agonist binding rate constant

The data presented above provide evidence that the α_1F64 mutation may affect both the binding process and gating properties of $\alpha_1\beta_1\gamma_2$ receptors, making the precise estimation of the impact of the mutation on specific rate constants difficult. To reduce the number of degrees of freedom, we applied a protocol that sought to determine the microscopic binding rate using the deconvolution-based "race" method (Jones et al., 1998; 2001). To this end, we first determined the rate constants that govern the competitive antagonism of GBZ. As described in Materials and Methods, the current responses to saturating [GABA] under control conditions and following pre-equilibration in GBZ

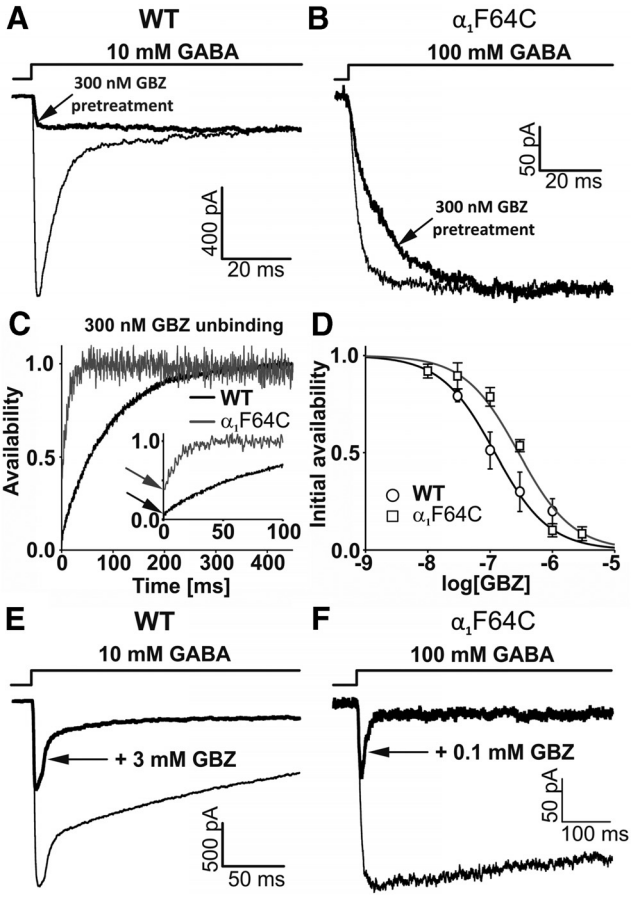

Figure 4. Estimation of the k_{on} rate constant using deconvolution based "race" method (see Materials and Methods) indicates that the α_1F64C mutation slows down the binding rate for GABA. ***A***, ***B***, Unbinding of the competitive antagonist (GBZ) decreased the current onset rate evoked by saturating [GABA]. The superimposed traces represent currents evoked by GABA alone (thin line) or the same GABA concentration following pretreatment with 300 nM GBZ (thick line) for wild-type (***A***, WT) and α_1F64C (***B***) receptors. ***C***, Time courses of receptor availability calculated by applying the deconvolution protocol to analyze traces evoked by saturating [GABA] with or without GBZ pretreatment (see Materials and Methods; black, WT receptors; gray, α_1F64C receptors). Plots were fitted with an exponential function that yielded the values of the unbinding time constants $\tau_{off\text{-}GBZ}$ and hence $k_{off\text{-}GBZ}$ (see Results for numerical values). In the lower inset, the same traces are shown in the expanded time scale. Arrows indicate availability at $t = 0$ (black for WT, gray for α_1F64C), used as a data points for fractional availability curve. ***D***, Fractional channel availability versus competitive antagonist concentration (circles, WT; squares, α_1F64C). Plots were fitted with the Hill equation (Eq. 1; Hill coefficient, 1), yielding the half occupancy KD-GBZ constant, and $k_{on\text{-}GBZ}$ was then calculated as the ratio of the unbinding rate $k_{off\text{-}GBZ}$ and KD-GBZ (see Results for numerical values). ***E***, ***F***, Typical current responses used in the race protocol evoked by saturating GABA application (thin line) and coapplication of saturating [GABA] and 3 mM GBZ (thick line) for WT (***E***) and 0.1 mM GBZ for α_1F64C mutants (***F***). Arrows indicate current response in GBZ presence. The current ratios (I_{race}) were used to estimate the agonist binding rate k_{on} (see Results for numerical values). The insets above the current traces indicate the application time of the specified compounds.

(Fig. 4*A*,*B*) were recorded, and the antagonist unbinding time course and initial availability were determined by deconvolution (Fig. 4*C*). The α_1F64C mutation substantially accelerated antagonist unbinding with respect to the wild-type receptors, determined by exponential fitting to the availability curves (wild type: $\tau_{off\text{-}GBZ}$, 102 ± 11 ms; $k_{off\text{-}GBZ}$, $9.8 \cdot 10^{-3} \pm 1.1 \cdot 10^{-3}$ ms^{-1}, $n = 11$; α_1F64C: $\tau_{off\text{-}GBZ}$, 20 ± 3 ms, $k_{off\text{-}GBZ}$, $50.3 \cdot 10^{-3} \pm 1.2 \cdot 10^{-3}$ ms^{-1}, $n = 7$; $p = 1.65 \cdot 10^{-5}$, unpaired t test). Initial GABA$_A$R availability was determined for a range of antagonist concentrations, and the dose–response relationships were constructed for both wild type and the α_1F64C mutant (Fig. 4*C*). The initial

availability curve (Fig. 4*D*) was best fitted with the Hill equation with Hill coefficient equaling 1, confirming previous observations (Jones et al., 1998, 2001; Wagner et al., 2004; Goldschen-Ohm et al., 2011) that the occupancy of just one binding site was sufficient for competitive inhibition by GBZ. As shown in Figure 4*D*, mutant receptors showed a rightward shift in the initial availability curve with respect to the wild-type channels (half-occupancy KD-GBZ: wild type, $1.2 \cdot 10^{-4}$ mM; α_1F64C, $2.9 \cdot 10^{-4}$ mM; Fig. 4*D*). The antagonist k_{on}, calculated as the ratio of the unbinding rate $k_{off\text{-}GBZ}$ and KD-GBZ, was slightly larger for α_1F64C (wild type, $k_{on\text{-}GBZ}$, 82 ± 9 mM^{-1}ms^{-1}; α_1F64C, $k_{on\text{-}GBZ}$, 176 ± 4 mM^{-1}ms^{-1}).

To estimate the agonist binding rate, we next needed to assess I_{race} (see Materials and Methods), which required application of the "race protocol" (i.e., coapplication of saturating GABA with GBZ, 3 mM for control, 0.1 mM for α_1F64C; I_{race}: wild type, 0.44 ± 0.02, $n = 4$; α_1F64C, 0.42 ± 0.04, $n = 5$; Fig. 4*E*,*F*). Having established the I_{race} values, Equation 7 was used to estimate the agonist binding rate. As expected, k_{on} was strongly reduced by the α_1F64C mutation (k_{on}: control, 9.9 ± 1.5 mM^{-1}ms^{-1}, $n = 4$; α_1F64C, 0.067 ± 0.012 mM^{-1}ms^{-1}, $n = 5$).

Effects of α_1F64 mutations on single-channel conductance and open probability: nonstationary variance analysis of GABA-evoked and pentobarbital-evoked currents

The variance (σ^2) and mean current amplitude (I) relationship was plotted for binning specified in Materials and Methods (Fig. 5*A–C*) for GABA-evoked traces, excluding current onset. A standard parabolic curve, $\sigma^2 = iI - I^2N^{-1} + c$, was fitted (Fig. 5*A*,*B*) and the single-channel current amplitude (i) was calculated (see Materials and Methods). Neither the α_1F64C nor α_1F64L mutation significantly affected single-channel conductance (g: wild type, 30 ± 3 pS, $n = 9$; α_1F64L, 32 ± 3 pS, $n = 4$; α_1F64C, 28 ± 3 pS, $n = 7$; Fig. 5*A–C*,*E*). However, whereas the parabolic fit could be reliably obtained for wild-type and α_1F64L mutant receptors (Fig. 5*A*,*B*) yielding the maximum open probability values ($P_{o\text{-}MAX}$: wild type, 0.67 ± 0.07, $n = 8$; α_1F64L, 0.61 ± 0.08, $n = 4$, $p = 0.58$; Fig. 5*F*), the variance–current relationship for α_1F64C mutants was basically linear, indicating low open probability (Fig. 5*C*) and precluding the determination of $P_{o\text{-}MAX}$. This important information, however, could be obtained from additional data derived from recordings of the currents elicited by PB.

PB at sufficiently high concentrations is known to activate $GABA_A$ receptors through a molecular pathway that is independent of the GABA binding site (Amin and Weiss, 1993; Drafts and Fisher, 2006; Mercado and Czajkowski, 2008; Venkatachalan and Czajkowski, 2008). Thus, we determined the responsiveness of the considered receptors to PB and performed the nonstationary variance analysis for PB-evoked currents. Because PB also potently blocks activated $GABA_A$Rs (Gingrich et al., 2009), the analysis was performed for so-called rebound currents that were observed upon PB removal (10 mM PB was applied for 100–500 ms; Fig. 6*A*). Single-channel conductance, determined for PB-evoked currents was indistinguishable from the single-channel conductance determined for GABA-activated currents for both wild-type receptors ($g = 34 \pm 3$ pS, $n = 4$, $p = 0.44$, compared with GABA-evoked conductance; Fig. 5*D*,*E*) and α_1F64C mutant receptors ($g = 33 \pm 4$ pS, $n = 4$, $p = 0.34$, compared with GABA-evoked conductance; Fig. 5*D*,*E*). Importantly, for both wild-type and α_1F64C mutant receptors, variance versus current plot could

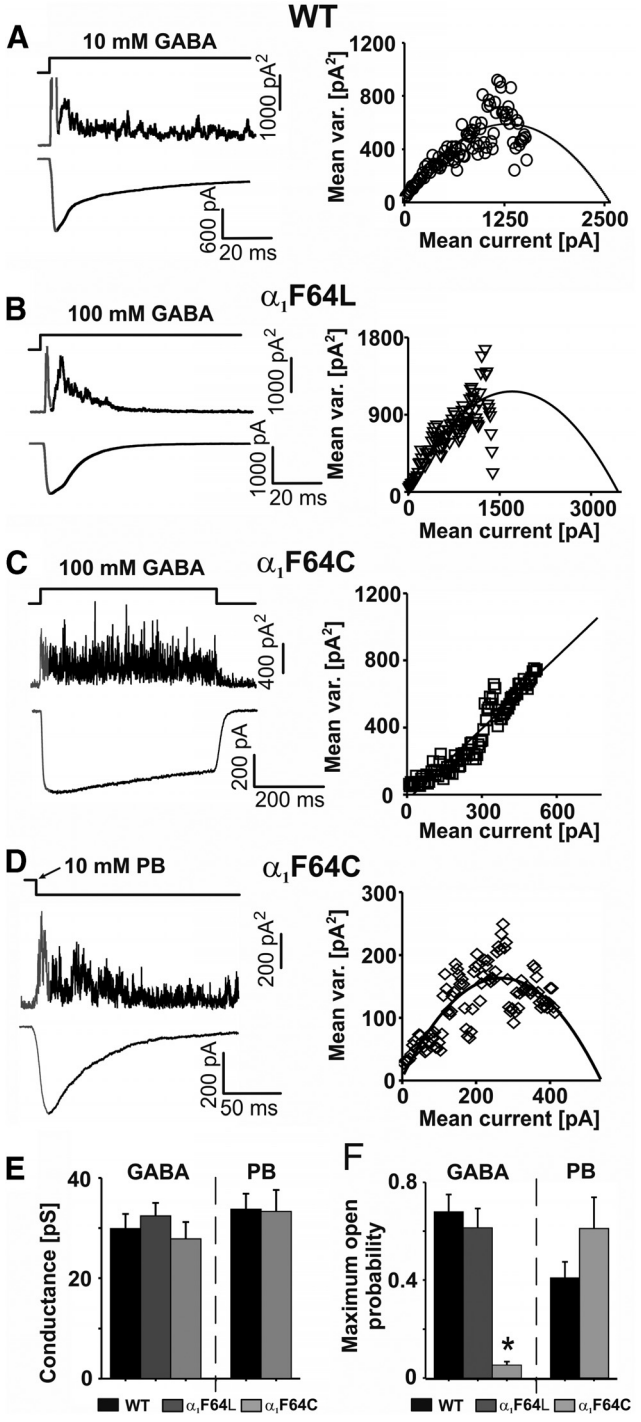

Figure 5. Nonstationary variance analysis shows that the α_1F64C mutation strongly decreases the maximum open probability but does not affect single-channel conductance. ***A–C***, Traces averaged from ≥10 consecutive current responses to saturating [GABA] mediated by wild-type (***A***, WT), α_1F64L (***B***), and α_1F64C (***C***) receptors aligned with plots that represent the variance of the current at each time point. The gray parts of the plots correspond to current onset, which was excluded from the analysis; see Results). ***D***, Plots analogous to those in ***A–C*** but for rebound currents observed upon the removal of 10 mM PB for α_1F64C receptors. On the right in ***A–D***, the respective current versus variance plots are shown. ***E***, Summary of values of single-channel conductance for GABA-evoked and PB-evoked currents (see Results for numerical values). ***F***, Statistics of maximum open channel probability values for GABA and PB (see Results for numerical values). The insets above the current traces indicate the application time of the specified agonist. The asterisk indicates a statistically significant difference.

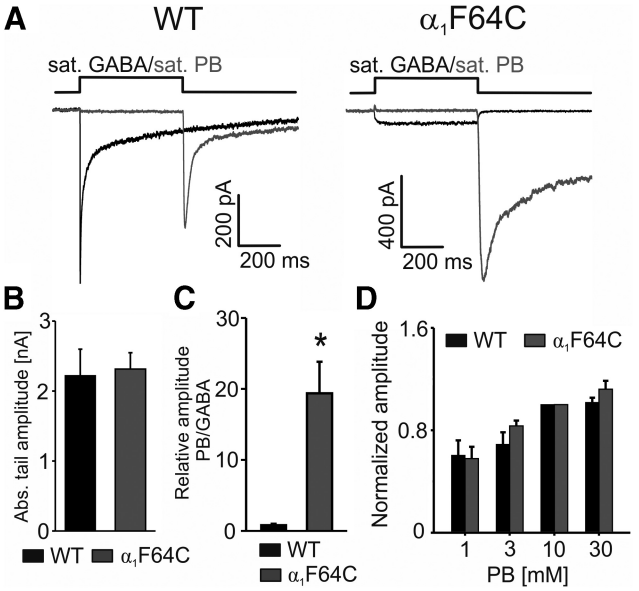

Figure 6. PB-evoked currents reveal that the α_1F64C mutation does not affect activation of GABA$_A$R by the pathway distinct from GABA-binding site. ***A***, Typical current responses to saturating concentrations of GABA-elicited (black) and PB-elicited tail currents (gray) mediated by wild-type (left, WT) and α_1F64C (right) receptors. ***B***, Statistics for amplitudes of PB-evoked currents mediated by WT (black bar) and α_1F64C (gray bar) receptors. ***C***, Statistics of current ratios for responses evoked by 10 mM PB and saturating [GABA] for WT (black bar) and α_1F64C (gray bar) receptors. PB-evoked currents mediated by WT and α_1F64C receptors had indistinguishable amplitudes, but GABA-evoked currents for α_1F64C mutant receptors were much smaller than for WT receptors. ***D***, Tail amplitudes normalized to the amplitude of the tail current evoked by 10 mM PB in the same cell for current responses to different concentrations of PB for WT and α_1F64C receptors. No difference was found between WT and α_1F64C mutants. The insets above the current traces indicate the application time of the specified agonist. Asterisks indicate a statistically significant difference.

be reliably fitted with a parabolic curve, and the $P_{o\text{-}MAX}$ parameters were determined ($P_{o\text{-}MAX}$: wild type, 0.41 ± 0.06, $n = 4$; α_1F64C, 0.61 ± 0.13, $n = 4$, $p = 0.21$, compared with wild type; Fig. 5*F*). Thus, when PB was used as the agonist, both wild-type and α_1F64C mutant receptors had high $P_{o\text{-}MAX}$ values that were comparable to the $P_{o\text{-}MAX}$ values estimated for responses evoked by saturating [GABA] in wild-type receptors.

Our finding that single-channel conductance was indistinguishable in both wild-type and α_1F64C mutant receptors determined from currents elicited by PB and GABA was helpful when estimating $P_{o\text{-}MAX}$ for GABA-evoked currents mediated by α_1F64C mutants. We first recorded the current response to saturating [GABA]. A series of PB-evoked rebound currents were then recorded from the same patch to perform the nonstationary variance analysis and calculate the $i \cdot N$ value. Dividing the maximum GABA-evoked current by $i \cdot N$ yielded the value of $P_{o\text{-}MAX}$ for α_1F64C receptors. Using this approach, we found that the α_1F64C mutation strongly reduced the $P_{o\text{-}MAX}$ value (α_1F64C: $P_{o\text{-}MAX} = 0.05 \pm 0.01$, $n = 3$, $p = 3.4 \cdot 10^{-5}$; Fig. 5*D*,*F*), providing additional evidence that this mutation interferes with receptor gating properties.

To further characterize the relationship between GABA-evoked and PB-evoked currents, we compared current responses to saturating [GABA] and rebound PB-evoked currents (Fig. 6*A*) measured from the same cells that expressed either wild-type or α_1F64C mutant receptors. Interestingly, the values of the tail current amplitudes measured for cells that expressed wild-type or α_1F64C mutant receptors did not show any significant difference (I_t: wild type, 2221 ± 377 pA, $n = 19$; α_1F64C, 2314 ± 234 pA, $n = 44$, $p = 0.83$, unpaired *t* test; Fig. 6*B*). This finding indicates that the mechanism of activation by PB was not markedly altered by the mutation, confirming previous data that PB does not affect the surface expression of these receptors (Petrini et al., 2011). For cells that expressed wild-type receptors, the ratio of PB-evoked and GABA-evoked currents was close to 1 (0.8 ± 0.2, $n = 4$; Fig. 6*C*). For α_1F64C mutants, the amplitude of the PB-evoked rebound current was dramatically larger than the amplitude elicited by saturating [GABA] (ratio: 19.4 ± 4.3, $n = 4$, $p = 0.023$; Fig. 6*C*). This result corroborates our conclusion based on the nonstationary variance analysis that the α_1F64C mutation strongly reduces the receptor's open probability when activated by GABA. Moreover, to further determine whether PB-induced activation is affected by the α_1F64C mutation, we constructed dose–response relationships for amplitudes of rebound currents normalized to the response to 10 mM PB and found no significant difference between wild-type and mutants receptors (Fig. 6*D*). Altogether, these results indicate that activation of the mutated receptor with PB circumvented the activation pathway that involves a mutated GABA binding site. Conversely, based on the aforementioned observations, we propose that the α_1F64 mutation affects receptor gating properties when its activation involves the GABA binding site.

The use of a partial agonist further indicates the effect of the α_1F64 residue mutation on receptor's apparent efficacy

The data presented above provide evidence that the α_1F64 residue mutation strongly interferes with receptor gating properties. However, gating may involve different conformational transitions, including opening/closing (efficacy) and desensitization processes. Moreover, recent studies emphasized the importance of nonconducting bound conformational transitions, termed flipping (Burzomato et al., 2004; Lape et al., 2008), priming (Mukhtasimova et al., 2009), and preopening (Jadey and Auerbach, 2012), that precede channel opening. In the remaining sections of the Results, we present our data using the classic convention (i.e., referring to binding, opening/closing efficacy, and desensitization). The section following Results is dedicated to model simulations. Then, in Discussion, we extensively discuss the impact of the flipping states. This form of presentation enables us to emphasize the drawbacks of using a classic approach and to stress the key role of flipping transitions in setting the relationship between microscopic receptor gating and the time course of measured current responses.

Based on the data presented above, it seems likely that the effects of the studied mutations on current kinetics and maximum open channel probability involve a reduction of receptor efficacy. To further test this hypothesis, we used the partial agonist piperidine-4-sulfonic acid (P4S), an agonist that activates the receptor with lower efficacy than GABA (Mortensen et al., 2004). As expected, rapid application of a saturating concentration of P4S (1 mM) elicited a current with a substantially smaller amplitude with respect to the response evoked by saturating [GABA] (P4S/GABA amplitude ratio, 0.27 ± 0.03, $n = 7$; Fig. 7*A*,*B*). In the case of α_1F64C mutant receptors, as with wild-type receptors, a saturating P4S concentration (10 mM) evoked currents with a markedly lower amplitude than saturating [GABA] (P4S/GABA amplitude ratio, 0.57 ± 0.02, $n = 5$; Fig. 7*A*,*B*), although the amplitude ratio was significantly ($p = 2.36 \cdot 10^{-5}$, unpaired *t* test) higher than the ratio for wild-type receptors (Fig. 7*B*). Interestingly, in addition to reduced amplitudes, responses to saturating concentrations of P4S were characterized by a significantly slower rise time compared with the responses evoked by

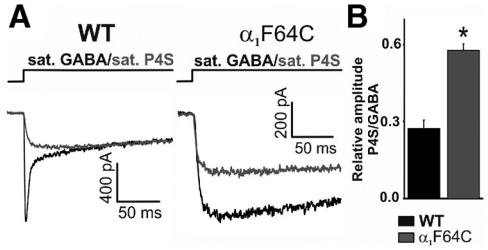

Figure 7. F64C mutation in the α_1 subunit of wild-type (WT) $GABA_ARs$ differentially affects the amplitude and kinetics of P4S-evoked and GABA-evoked currents. ***A***, Typical traces of current responses elicited by long (500 ms) applications of saturating concentrations of GABA and P4S in WT (left) and α_1F64C (right) receptors. In the currents evoked by saturating [P4S] and mediated by WT receptors, no rapid desensitization component was present. ***B***, Relative amplitudes of currents evoked by saturating [P4S] and [GABA] for both types of receptors. P4S-evoked and GABA-evoked currents were collected each time from the same patch and therefore paired test was applied (≥5 cells in statistics). The insets above the current traces indicate the application time of the specified agonist. The asterisk indicates a statistically significant difference.

saturating [GABA] in wild-type receptors (t_{Rise} for P4S relative to GABA: 15.8 ± 1.8, $n = 3$, $p = 0.004$, unpaired t test,), but not in α_1F64C mutant receptors relative to GABA (t_{Rise} for P4S relative to GABA: 1.1 ± 0.4, $n = 5$, $p = 0.64$, unpaired t test). Notably, currents mediated by wild-type receptors and elicited by saturating P4S showed a similar kinetic phenotype as GABA-evoked responses recorded from cells that expressed α_1F64C mutant receptors (Fig. 7*A*). In P4S-evoked responses mediated by wild-type receptors, the rapid desensitization component virtually disappeared [FR(10): GABA, 0.43 ± 0.05, $n = 6$; P4S, 0.93 ± 0.03, $n = 6$; $p = 4.41 \cdot 10^{-5}$; Figure 7*A*] and the onset kinetics were much slower than for GABA-evoked currents. This finding raises the possibility that an alteration of receptor's apparent efficacy might be a major mechanism whereby the α_1F64 mutation alters receptor gating. Moreover, considering this observation, the lack of a rapid fading component in current responses mediated by α_1F64C mutants does not necessarily indicate that this mutation interferes with the molecular mechanisms that determine desensitization (Bianchi and Macdonald, 2003; Mozrzymas et al., 2003a).

Differential impact of α_1F64mutations on the kinetics of GABA-evoked and muscimol-evoked currents

In the preceding section, we reported that the kinetics of currents mediated by α_1F64C mutants and evoked by saturating [GABA] were strikingly similar to responses mediated by wild-type $GABA_ARs$ elicited by saturating P4S. However, as described above, this mutation also strongly affects receptor binding characteristics. To better distinguish between the effect of the mutation on binding properties and the effect of the mutation on gating properties, we performed recordings using muscimol, an agonist that has been shown to have a higher apparent affinity than GABA, presumably because of a slower unbinding rate constant (Jones et al., 1998). This mechanism might predict that currents evoked by muscimol would be characterized by slower deactivation kinetics compared with GABA-evoked currents. We verified that the saturating concentrations of muscimol were 1 mM for wild type, 3 mM for the α_1F64L mutation, and 30 mM for the α_1F64C mutation. As shown in Figure 8*A*,*B*, for wild-type receptors, deactivation τ_{mean} was >2-fold larger for muscimol-induced currents (relative $\tau_{mean\text{-}MSC}/\tau_{mean\text{-}GABA}$, 2.87 ± 0.41, $n = 8$, $p = 0.002$). Interestingly, for the α_1F64L mutation, the deactivation kinetics of GABA-evoked currents were very fast (Figs. 2*B*,

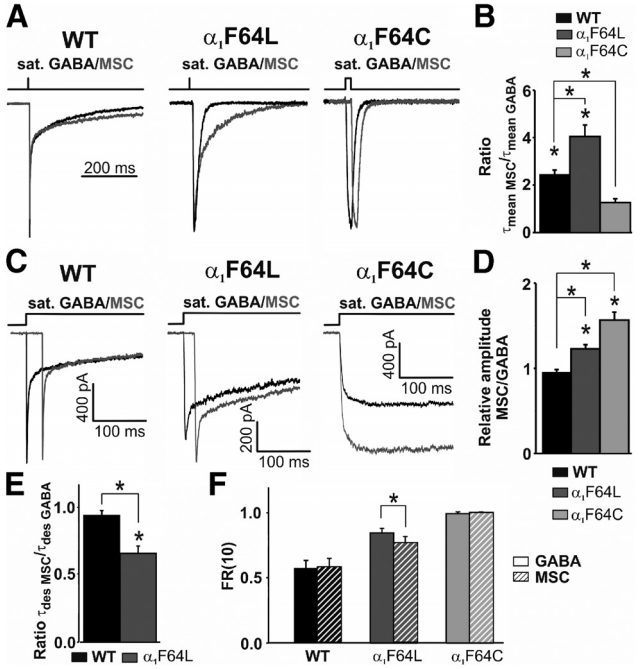

Figure 8. Leucine and cysteine mutations at the α_1F64 residue differentially affect the amplitudes and kinetics of muscimol-evoked currents. ***A***, Normalized and superimposed current responses for short applications of saturating concentrations of muscimol (gray) and GABA (black) for wild-type (WT), α_1F64L, and α_1F64C receptors. Because the considered mutations slowed the onset kinetics (Fig. 3), the durations of the agonist application times were chosen to include the entire rising phase of the responses and their peak/maximum values: WT, 3–5 ms; α_1F64L, 8–15 ms; α_1F64C, 10–30 ms. The saturating concentrations of muscimol were as follows: 1 mM for WT, 3 mM for α_1F64L, and 30 mM for α_1F64C. ***B***, Statistics for relative mean deactivation time constant $\tau_{mean\text{-}MSC}/\tau_{mean\text{-}GABA}$ for currents evoked by short applications of saturating concentrations of muscimol and GABA in three types of receptors. Statistically significant differences were found between GABA-elicited and muscimol-elicited currents in WT and α_1F64L, but not in α_1F64C. ***C***, Typical superimposed traces of current responses to long (500 ms) applications of saturating concentrations of GABA and muscimol mediated by WT, α_1F64L, and α_1F64C receptors. WT and α_1F64L muscimol responses were time-offset for presentation clarity. ***D***, Statistics of amplitude ratios for responses evoked by saturating [GABA] and [muscimol] for the specified receptors. Statistically significant increases in the amplitude ratios were observed for both mutated receptors (paired t test, $n \geq 6$), indicating greater muscimol efficacy (see Results and Discussion). ***E***, Summary of relative values of rapid desensitization time constant (τ_{des}) for current responses to long applications of saturating [muscimol] and [GABA] in WT and α_1F64L receptors. ***F***, Statistics of fraction of current remaining 10 ms after reaching a maximum value for responses to GABA (first bar) and muscimol (second bar) mediated by WT, α_1F64L, and α_1F64C receptors. In the case of currents mediated by α_1F64L receptors, muscimol induced faster desensitization than GABA, but this was not the case for α_1F64C receptors. For the data presented in ***E*** and ***F***, a paired t test was used ($n \geq 6$). The insets above the current traces indicate application time of the specified agonist. The asterisk indicates a statistically significant difference.

8*A*). When muscimol was applied, τ_{mean} was prolonged >4-fold (relative $\tau_{mean\text{-}MSC}/\tau_{mean\text{-}GABA}$, 4.42 ± 0.37, $n = 10$, $p = 3 \cdot 10^{-5}$; Fig. 8*A*,*B*). However, in the case of the α_1F64C mutation, when muscimol was applied, the deactivation kinetics remained nearly as fast as for GABA-evoked currents (relative $\tau_{mean\text{-}MSC}/\tau_{mean\text{-}GABA}$, 1.27 ± 0.16, $n = 4$, $p = 0.076$, paired t test; Fig. 8*A*,*B*). Fitting with the Hill equation (Eq. 1) yielded an EC_{50} of 897 μM ($n_h = 0.8$), which is less than one-seventh of EC_{50} for GABA (see above). To provide evidence that apparent affinity for muscimol is larger than for GABA also for α_1F64C mutants, we determined the dose–response relationship for muscimol (data not shown). Fitting with the Hill equation (Eq. 1) yielded an EC_{50} of 897 μM ($n_h = 0.8$) i.e., >7-fold lower than in the case of GABA (see above). In the case of wild-type receptors, amplitudes of GABA-

evoked currents were virtually the same as those of muscimol-evoked currents ($I_{MSC}/I_{GABA} = 0.95 \pm 0.03$, $n = 7$, $p = 0.31$, saturating agonists; Fig. 8*C*,*D*). Moreover, the macroscopic fast desensitization determined for currents evoked by muscimol and GABA did not significantly differ (relative: $\tau_{des\text{-}MSC}/\tau_{des\text{-}GABA} = 0.96 \pm 0.03$, $n = 8$, $p = 0.23$; Fig. 8*E*), which is consistent with previous reports (Jones et al., 1998). However, surprisingly, in the case of the α_1F64L mutants, the amplitude of muscimol-evoked currents was significantly larger than for GABA-evoked currents ($I_{MSC}/I_{GABA} = 1.23 \pm 0.05$, $n = 10$, $p = 0.003$; Fig. 8*C*,*D*). This observation suggests that for this mutant, muscimol not only has a larger affinity but also activates the receptor with greater efficacy. Moreover, when α_1F64L mutant receptors were activated by muscimol, both the desensitization time constant (relative: $\tau_{des\text{-}MSC}/\tau_{des\text{-}GABA} = 0.67 \pm 0.06$, $n = 9$, $p = 0.002$; Fig. 8*E*) and FR(10) parameter were significantly smaller than those for GABA-evoked currents [$FR(10)_{relative} = 0.90 \pm 0.02$, $n = 10$, $p = 0.0003$; Fig. 8*C*,*F*], indicating a larger rate and extent of desensitization in the case of activation by muscimol. Similar to α_1F64L, currents mediated by α_1F64C mutants and evoked by saturating [muscimol] showed a markedly larger amplitude compared with responses elicited by GABA ($I_{MSC}/I_{GABA} = 1.57 \pm 0.10$, $n = 6$, $p = 0.034$, compared with wild type, paired t test; Fig. 8*C*,*D*). However, no rapid desensitization component was present in either GABA-evoked or muscimol-evoked responses mediated by these mutants (Fig. 8*C*,*F*). Overall, these results show that muscimol appears to differ from GABA in wild-type receptors mainly in apparent affinity, but in the case of mutants, it activates these receptors with a markedly larger apparent efficacy. Thus, these mutations render receptor gating sensitive to the identity of these agonists.

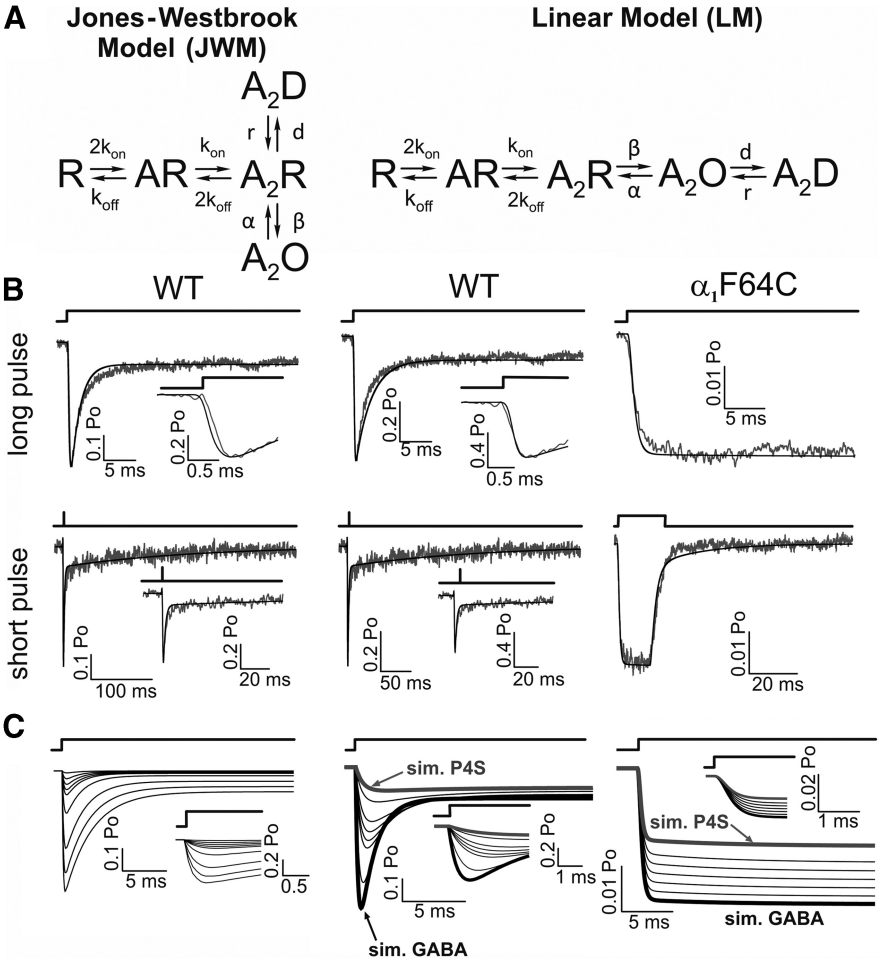

Figure 9. Model simulations based on classic JWM and LM. ***A***, Kinetic schemes used to fit experimental data. Left, JWM (Jones and Westbrook, 1995). Right, LM (Bianchi et al., 2007). ***B***, Exemplary fits (black line) to experimental current responses (gray line) to long (upper row) and short (lower row) applications of saturating GABA for (left to right) the JWM fit to wild-type (WT) receptor-mediated currents, and the linear model fit to WT receptor-mediated and α_1F64C mutant receptor-mediated currents. The JWM mechanism was not fitted to mutant receptor-mediated currents because of qualitative discrepancies (see Results, Model simulations). The figure shows that the fits of both models were made for the same representative current responses for WT receptors. For kinetic rate constants, see Table 1. ***C***, Curve families for each of the two models generated by lowering the opening rate constant β (decrease in efficacy) starting from the value obtained from fitting current responses mediated by WT receptors. The modeled GABA application represented by a thick black line, and P4S is represented by a thick gray line. Left to right, JWM for WT receptors, LM for wild-type receptors, and LM for α_1F64C mutants. In the case of the JWM, decreasing efficacy could not account for the loss of fast macroscopic desensitization when saturating partial agonist, whereas the LM correctly predicted the loss of rapid desensitization and slowing of the current onset upon a decrease in efficacy. For β values established for α_1F64C mutant receptors, a further lowering of β led to a decrease in amplitude but not any substantial prolongation of rise time (***C***, right, curve family; see also Results, Model simulations). The insets above the current traces indicate the application time of the specified agonist. Notice that for F64C mutant P4S application fit, there is additional small shift of α value (Table 2). For experimental and simulated parameters, see Tables 1 and 2.

Model simulations

The experimental data presented above show that α_1F64 mutations strongly affect both the binding and gating of $\alpha_1\beta_1\gamma_2$ receptors. The application of the racing procedure enabled us to estimate the impact of this mutation on the binding rate, but its effect on specific gating characteristics remains obscure. To gain further insights into this issue, we applied kinetic simulations (see Materials and Methods) to test the predictions of different minimum requirement models. Because the vast majority of our recordings were made either for saturating or high ($>EC_{50}$) agonist concentrations at which the occupancy of singly bound states is expected to be minimal, these states were omitted. Slow desensitization components were also not considered; for this reason, fits to recorded current traces for protocols with prolonged ligand applications were restricted to the first 15–30 ms, a time period during which the rapid desensitization component was predominant. As mentioned above in the Results, we first attempted to fit our data using classic models (Fig. 9*A*, JWM and LM) and subsequently extended these investigations to models that included the flipped state (Fig. 10*A*, fJWM and fLM). Our fitting procedure was designed to optimally fit the kinetic shape of individual currents and reproduce major differences between wild-type and mutant receptors by using the simplest possible models and manipulating the minimum number of rate constants.

We first used the JWM (Fig. 9*A*), which has been shown to reproduce major kinetic features of GABA$_A$Rs (Jones and Westbrook, 1995; Mozrzymas et al., 1999). Our present data collected

Table 1. Experimental and model-predicted current parameters and rate constants for GABA-evoked responses mediated by wild-type (WT) and α1F64C mutant receptors

	Experimental			LM			fJWM			fLM		
Current parameter[a]	WT	αF64C	Ratio	WT	αF64C	Ratio	WT	αF64C	Ratio	WT	αF64C	Ratio
Deactivation τ_{mean} (ms)	25.9	1.5	0.06	11.4	2.3	0.2	25.4	1.3	0.05	31.5	1.8	0.06
FR(10)	0.29	0.93	3.24	0.22	1	4.55	0.19	1	5.26	0.29	1	3.45
10–90% onset (ms)	0.25	1.12	4.48	0.24	0.75	3.13	0.29	1.51	5.21	0.37	0.6	1.62
$P_{o\text{-}MAX}$	0.67	0.05	0.08	0.62	0.03	0.05	0.25	0.01	0.03	0.52	0.04	0.07
EC_{50} (mM)	0.071	6.6	92.96	0.131	17.9	136.64	0.156	24.2	155.13	0.142	27.6	194.37
	JWM											
	WT			LM			fJWM			fLM		
Rate constant[b]				WT	αF64C	Ratio	WT	αF64C	Ratio	WT	αF64C	Ratio
k_{on} (mM^{-1}ms^{-1})	9.9 ± 1.5			9.9 ± 1.5	0.067 ± 0.012	0.01	9.9 ± 1.5	0.10	0.01	9.9 ± 1.5	0.09	0.01
k_{off} (ms^{-1})	330 ± 60			0.52 ± 0.14	0.52	1	1.16 ± 0.10	1.16	1	1.30 ± 0.32	1.3	1
δ (ms^{-1})	—			—	—	—	4.03 ± 0.21	0.27 ± 0.04	0.07	3.53 ± 0.85	1.87 ± 0.40	0.53
γ (ms^{-1})	—			—	—	—	4.46 ± 1.74	195 ± 7	43.72	1.53 ± 0.23	60.6 ± 14.9	40
β (ms^{-1})	7.67 ± 1.96			4.63 ± 0.76	0.14 ± 0.03	0.03	16.5 ± 8.9	16.5	1	9.89 ± 3.40	10.2 ± 2.3	1.03
α (ms^{-1})	1.03 ± 0.11			0.77 ± 0.22	3.21 ± 0.37	4.17	1.69 ± 0.20	1.69	1	1.02 ± 0.19	4.18 ± 0.76	4.1
d (ms^{-1})	5.27 ± 1.33			0.82 ± 0.13	0.82	1	23.8 ± 10.2	28.8 ± 5.2	1.21	1.04 ± 0.18	1.04	1
r (ms^{-1})	0.07			0.14 ± 0.01	0.14	1	0.12 ± 0.01	0.21 ± 0.10	1.75	0.18 ± 0.02	0.18	1

[a]Comparison between current parameters measured experimentally and those predicted by different models. Kinetic parameters (specified in the first column) are presented as absolute values in respective units. The parameters' ratio (α1F64C to wild type) are given in the Ratio columns.

[b]Rate constants optimized for all kinetic schemes for WT and α1F64C receptors. In the third column for different models, the ratios of specific parameters for α1F64C and WT are specified. The values are presented for 10 mM GABA for WT and 100 mM GABA for α1F64C.

Table 2. Experimental and model-predicted current parameters and model rate constants for P4S application in wild-type (WT) and α1F64C mutant receptors

	Experimental		LM		fJWM		fLM	
Parameter	WT	αF64C	WT	αF64C	WT	αF64C	WT	αF64C
Amplitude ratio	0.27	0.57	0.22	0.57	0.19	0.57	0.25	0.58
Onset ratio	15.8	1.1	4.4	1.1	5.4	1.1	5.9	1.3
FR(10) for P4S application	0.93	1	0.89	1	0.91	1	1	1
Rate constant change relative to GABA application			β, 0.043	β, 0.64; α, 1.24	δ, 0.040	δ, 0.55	δ, 0.056	δ, 0.53

The amplitude and onset ratios represent the values obtained for P4S relative to those measured for GABA. In the case of FR(10), the absolute values are reported. The bottom row specifies the rate constant that had to be changed with respect to those optimized for GABA-evoked currents to reproduce the time course of currents evoked by P4S. The numbers to the right of the rate constant symbols represent the coefficients by which respective rate constants optimized for GABA-evoked currents should be multiplied to reproduce responses elicited by P4S.

for wild-type receptors confirmed the validity of this model because optimization of its rate constants (Table 1) yielded a satisfactory fit to current responses elicited by various protocols of GABA applications (Fig. 9*B*). However, surprisingly, this model failed to reproduce our major observations for currents evoked by a partial agonist (P4S) and currents mediated by the mutants. Assuming that P4S activates GABA$_A$Rs with lower efficacy than GABA, we attempted to fit this model to the recorded traces (saturating P4S) by manipulating the α or β rate constants over a wide range, assuming that α must be larger for P4S than for GABA, as deduced from single-channel data (Mortensen et al., 2004). However, we failed to concomitantly reproduce the lack of rapid macroscopic desensitization as experimentally shown in Figure 2*E* (compare with Fig. 7*A*) and slow current onset together with the amplitude reduction (Fig. 9*C*). A reasonable reproduction of the current time course evoked by high [P4S] could be approached only when the reduction of the unbinding rate (k_{off}) was so strong that the modeled responses escaped the saturation. When considering this model, we encountered yet another discrepancy when trying to reproduce our observations for mutants activated by GABA or muscimol. A larger amplitude of currents elicited by muscimol (with respect to GABA) in the case of α_1F64L mutants indicates that muscimol has not only a higher affinity but also a larger efficacy for these receptors. We thus tried to manipulate the rate constants that govern efficacy (β, α). However, contrary to our experimental findings (Fig. 8*C*), increased efficacy (muscimol vs GABA) resulted in a slowing of current fading upon prolonged agonist application. To correct this discrepancy, we enhanced the desensitization rate, resulting in a decrease in amplitude, in contrast to the experimental results. Altogether, although the JWM correctly reproduced the kinetic behavior of wild-type receptors, it failed to qualitatively reproduce our basic observations for the partial agonist and mutants.

Among the minimum requirement models of GABA$_A$Rs, the LM (Fig. 9*A*) has been considered a possible alternative to the JWM (Bianchi et al., 2007). Using this model, we correctly reproduced the kinetics of currents mediated by wild-type receptors and evoked by GABA (Fig. 9*B*, Table 1). Moreover, in contrast to the JWM, the LM satisfactorily predicted the major kinetic features of currents elicited by the application of the partial agonist P4S (it was sufficient to decrease the opening rate constant β; Fig. 9*C*, Table 2): including a decrease in amplitude, prolongation of the rise time, and acceleration of deactivation (Table 2). Importantly, the reduction of the opening rate β in the LM led to a decrease in the rate and extent of macroscopic desensitization. At sufficiently small β, this desensitization component eventually disappeared (Fig. 9*C*), which was observed in the experiments with P4S (Fig. 7*A*). This model also offered a good fit to the experimental data obtained for α_1F64C mutant receptors (Table 1). For responses elicited by the application of saturating agonists, the manipulation of receptor efficacy parameters, especially β, was sufficient to reproduce all of the major features of these currents (Fig. 9*B*, Table 1). Moreover, a further decrease in β led to a reduction of amplitude but produced a minor prolongation of the rise time, in contrast to the experimental observations for α_1F64C mutants. This discrepancy could be corrected by slightly

Table 3. Rate constants optimized to reproduce the kinetics of GABA-evoked current responses mediated by α1F64L receptors[a]

	LM	fJWM	fLM
β (ms^{-1})	2.9	16.5	9.89
α (ms^{-1})	1.9	1.69	1.02
δ (ms^{-1})	—	2.2	2.5
γ (ms^{-1})	—	20	9

[a]Only rate constants that were altered with respect to the model optimized for wild-type receptors (Table 1) are specified.

increasing the α rate constant (compare Figs. 7*A*, 9*C*). We next tested whether this model can reproduce the features of currents induced by muscimol. For wild-type receptors, good reproduction of the data could be obtained by lowering k_{off}, as suggested by Jones et al. (1998, 2001; see Table 4). Thus, by reducing k_{off}, deactivation was prolonged to a similar extent as in our experiments, whereas the fading of responses to prolonged muscimol application was unaltered with respect to GABA. To fully account for the effects of muscimol observed for α_1F64C and α_1F64L receptors (Table 3, manually optimized rate constants), we needed to additionally alter the rate constants that govern receptor efficacy (Table 4). This was sufficient to obtain a reasonable qualitative reproduction of our data (muscimol vs GABA), including a substantial increase in the deactivation time constant for α_1F64L receptors, an increase in amplitude for α_1F64C and α_1F64L receptors, and an increase in the rate and extent of desensitization for α_1F64L receptors (simulations not shown; Fig. 8, data). Thus, in contrast to the JWM, the LM qualitatively reproduced our major findings. However, some points may cast doubt on the appropriateness of this gating mechanism. First, the above interpretation would imply that the α_1F64 mutation qualitatively changes the muscimol-induced activation mechanism. Namely, it is well established that in γ_2 subunit-containing wild-type receptors, muscimol shows different apparent binding kinetics with respect to GABA (decreased unbinding; Jones et al., 1998, 2001; Mortensen et al., 2010), whereas for the mutants studied here the efficacy would also have to be affected. Although such an effect of the α_1F64 mutation cannot be excluded, it seems more probable that the general mechanism of agonist action remains similar in wild-type and mutant receptors. Second, several previous experimental observations argue against a purely linear arrangement for $GABA_AR$ gating. PB at potentiating concentrations increases GABA-evoked currents by increasing opening efficacy (Twyman et al., 1989; Feng et al., 2004), but decreases the extent of macroscopic desensitization (Feng et al., 2004), which requires a branched model. Moreover, for mutations that uncouple desensitization from deactivation (Bianchi et al., 2007), an increase in efficacy is not accompanied by an increase in macroscopic desensitization as expected in the LM. Additionally, Scheller and Forman (2002) studied the uncoupling of efficacy and desensitization in a pore domain mutant (α_1L264T) that exhibited increased efficacy and a significant loss of macroscopic desensitization, consistent with reduced occupancy of the desensitized state. However, currents mediated by these receptors also had prolonged deactivation, which is problematic to reproduce using the LM.

The major conceptual problem when attempting to interpret our data is that mutation of the residue localized at the binding site strongly affects receptor gating, especially rate constants that determine efficacy, which is believed to mainly depend on structures localized at the transmembrane domain or at the interface between transmembrane and extracellular domains (Cederholm et al., 2009; Miller and Smart, 2010; Bouzat, 2012). In the past decade, however, a novel concept emerged, in which energy provided by agonist binding induces some conformational changes (flipping, preopening, or priming) that precede channel opening (Burzomato et al., 2004; Auerbach, 2005; Lape et al., 2008, 2012; Mukhtasimova et al., 2009; Colquhoun and Lape, 2012; Jadey and Auerbach, 2012). Clearly, alterations induced by an agonist at the binding site cannot be transmitted with light velocity to the channel gate; instead a "Brownian conformational wave" is expected to occur (Auerbach, 2005).

Therefore we adopted the concept of flipping in our investigations by considering two additional schemes (Fig. 10*A*), including a transitional state between a fully bound closed state and opening/desensitization conformations. fJWM is an extension of JWM, and fLM represents an analogous modification of LM. Both fJWM and fLM produced a good fit to the wild-type receptor data (Table 1), and the differences in their predictions were minor. The fJWM predicted low $P_{o\text{-}MAX}$, and the fLM predicted a slower rise time than the one measured experimentally. We then tried to establish whether changes in flip rate constants can account for the kinetic phenotype observed in experiments with the partial agonist P4S. We simulated current responses for a broad range of δ and γ rate constants. For both models, predicting a concomitant decrease in amplitude and lack of rapid macroscopic desensitization was possible (Fig. 10*B*, Table 2). Interestingly, however, the two schemes showed qualitatively different desensitization dependence on the flip rate constants. Indeed, as shown in the surface plots in Figure 10*B*, desensitization depends mainly on δ in the fJWM, but qualitatively different dependence on both γ and δ occurs in the fLM. One interesting line of investigation would be to consider other mutations that affect the flipping transitions to verify the trends postulated by these models.

We then used the flipped models (Fig. 10*A*) to fit the responses mediated by α_1F64C receptors. Interestingly, in the case of the fJWM, the best fits were obtained by a large modification of the flip rate constants with respect to wild type, and only a relatively small correction of desensitization parameters was needed, which was not critical for qualitatively reproducing the current kinetics (Table 1). In the case of the fLM, manipulations restricted to the δ and γ rate constants were insufficient to obtain good fits, even at the qualitative level. The reproduction of fast deactivation kinetics for currents mediated by α_1F64C receptors additionally required adjustments of the α and β rate constants, whereas a good fit to the experimental data with the fJWM was obtained with the same α and β rate constants as for wild-type receptors (Table 1).

Importantly, a potential drawback of this approach is the reliance on k_{on} values determined using the racing protocol, assuming a model without flipping states (Jones et al., 1998). Indeed, the consideration of flipping states in the model may affect the estimation of binding parameters (Colquhoun and Lape, 2012). To assess the correction in the estimation of k_{on} caused by inclusion of a flipped state, we ran simulations in which k_{on} was optimized (the other parameters remained the same as in Table 1) to best reproduce the I_{race} value determined experimentally. This procedure did not affect the estimation of k_{on} for wild-type receptors and yielded only subtle changes in k_{on} values in the case of α_1F64C receptors (k_{on}: fJWM, 0.1 $mM^{-1} \cdot ms^{-1}$; fLM, 0.09 $mM^{-1} \cdot ms^{-1}$; compared with the previously determined k_{on} = 0.067 $mM^{-1} \cdot ms^{-1}$), and their overall impact on our simulations was negligible.

To further test the models that involved a flipped state, we determined whether it could reproduce the effects of muscimol in

Table 4. Experimental and model-predicted current parameter ratios and model rate constants for currents elicited by muscimol

Kinetic parameter relative to GABA application[a]	Experimental			LM			fJWM			fLM		
	WT	αF64C	αF64L	WT	αF64C	αF64L	WT	αF64C	αF64L	WT	αF64C	αF64L
Amplitude	0.95	1.57	1.23	1	1.35	1.23	1.03	1.48	1.2	1.04	1.81	1.28
τ_{des}	0.96	—	0.67	1	—	0.82	0.96	—	0.81	0.94	—	0.71
FR(10)	0.97	1	0.9	1	0.98	0.85	0.97	0.98	0.86	0.99	0.84	0.79
Deactivation τ_{mean}	2.87	1.27	4.42	3.04	2.11	5.09	2.91	1.26	4.56	2.93	1.19	3.37
				LM			fJWM			fLM		
Rate constant[b]				WT	αF64C	αF64L	WT	αF64C	αF64L	WT	αF64C	αF64L
k_{on} (m_M^{-1} ms^{-1})				9.9	0.067	na	9.9	0.10	na	9.9	0.09	na
k_{off} (ms^{-1})				0.15	0.15	0.15	1.16	1.16	1.16	1.30	1.30	1.3
δ (ms^{-1})				—	—	—	4.03	0.27	2.20	3.53	1.87	2.5
γ (ms^{-1})				—	—	—	1.50	120	4.00	0.50	30	2
β (ms^{-1})				4.63	0.14	3.80	16.5	16.5	16.5	9.89	10.2	9.89
α (ms^{-1})				0.77	3.21	1.70	1.69	1.69	1.69	1.02	4.18	1.02
d (ms^{-1})				0.82	0.82	0.82	23.8	28.8	23.8	1.04	1.04	1.04
r (ms^{-1})				0.14	0.14	0.14	0.12	0.21	0.12	0.18	0.18	0.18
Rate constant change relative to GABA application[c]				k_{off}, 0.28	k_{off}, 0.28; β, 1.07; α, 0.87	k_{off}, 0.288; β, 1.31; α, 0.89	γ, 0.33	γ, 0.61	γ, 0.2	γ, 0.32	γ, 0.49	γ, 0.22

[a]Kinetic parameter ratios for responses elicited by muscimol and GABA applications.

[b]Summary of rate constants optimized for muscimol application for different kinetic schemes.

[c]Rate constants changed with respect to those optimized for GABA-evoked currents to reproduce responses evoked by muscimol. The numbers represent the coefficients by which the respective rate constants optimized for GABA-evoked currents should be multiplied to reproduce kinetic characteristics of responses evoked by muscimol.

na, Rate constant value was not assessed.

the considered receptors. Surprisingly, for wild-type receptors, all of the major effects of muscimol (i.e., prolongation of deactivation time course and lack of effect on desensitization kinetics) could be well reproduced by decreasing the γ rate constant in both models (Fig. 10*C*, Table 4). Similarly, for α_1F64C, manipulating only the γ rate constant was sufficient to properly mimic our experimental observations, including an enhanced amplitude with no effect on desensitization and only weak slowing of deactivation (Fig. 10*D*, Table 4). Moreover, the effects of the α_1F64L mutation on currents evoked by GABA could be well reproduced by altering the flip constants alone (Fig. 10*E*, Table 4). Additionally, for this mutant, modification of the γ rate constant was sufficient to replicate the major differences in currents evoked by muscimol (Table 4). Altogether, both models that included a flipped state could properly reproduce all of the major features of the recorded currents for both wild-type and mutant receptors. However, the fJW model tended to be more accurate in predicting the kinetic features of the recorded currents (Tables 1, 2, 4). Most importantly, the consideration of these models allows us to conclude that the kinetics of responses elicited by the partial agonist P4S differed from the kinetics for GABA-evoked currents, mainly because of distinct flipping kinetics, and that mutation of the α_1F64 residue altered receptor gating by affecting flipping transitions.

Discussion

We provide evidence that α_1F64, a key aromatic residue at the GABA binding site, is involved in both the binding and gating properties of $\alpha_1\beta_1\gamma_2$ receptors. Importantly, major kinetic features (i.e., onset, deactivation, and macroscopic desensitization; Figs. 2, 3) were dramatically affected by mutations of this residue and the impact of α_1F64 mutation on receptor gating was further supported by a strong decrease in the channel open probability (Fig. 5). Previous studies focused mainly on the role of α_1F64 in binding properties with only some indirect suggestions of its involvement in gating (Sigel et al., 1992; Holden and Czajkowski, 2002). Holden and Czajkowski (2002) used a cysteine substitution method to show that PB-induced activation structurally rearranged a part of the binding site that contained α_1F64. The role of homologous residues in the D loop has been more extensively studied in other cys-loop receptors (Fig. 1*A*). In AChRs, these residues were suggested to affect gating (Xie and Cohen, 2001; Akk, 2002; Bafna et al., 2009). In particular, the notion of Bafna et al. (2009) that these mutations change open state affinity appears to be consistent with the hypothesis that they affect preopening transitions, resulting in a conversion from low to high affinity states (Lape et al., 2008; Colquhoun and Lape, 2012). Importantly, Jadey and Auerbach (2012) recently proposed a "catch-and-hold" mechanism that postulates that binding and affinity changes represent an integrated process that occurs in the early stage of activation. This mechanism appears to be compatible with the concept of flipping states (Lape et al., 2008; Colquhoun and Lape, 2012) or priming (Mukhtasimova et al., 2009). No apparent effects on gating were observed for mutations in homologous 5-HT$_3$Rs (Spier and Lummis, 2000) or $\alpha_4\beta_3\delta$ GABA$_A$Rs (Absalom et al., 2012). Mutation of a homologous residue in ρ homomeric GABA$_A$Rs induced spontaneous activity (Torres and Weiss, 2002), supporting the hypothesis that residues at this position are important for gating across the cys-loop receptor family. Notably, most previous studies did not address the impact of these mutations on gating components other than opening or closing because apparently nondesensitizing receptors were studied or because solution exchange was too slow to reveal fast desensitization. In the present study, the most marked effect of α_1F64 mutations was the suppression of rapid macroscopic desensitization (Fig. 2). The only similar observation was reported by a study on homomeric α_7 AChRs in which a homologous mutation slowed desensitization onset (Gay et al., 2008). In contrast to GABA$_A$Rs, however, no effect on binding or on gating parameters other than desensitization was reported. The strong effect of the α_1F64 mutation on rapid desensitization is puzzling because most studies in which the structural determinants of this process were investigated indicated residues in transmembrane

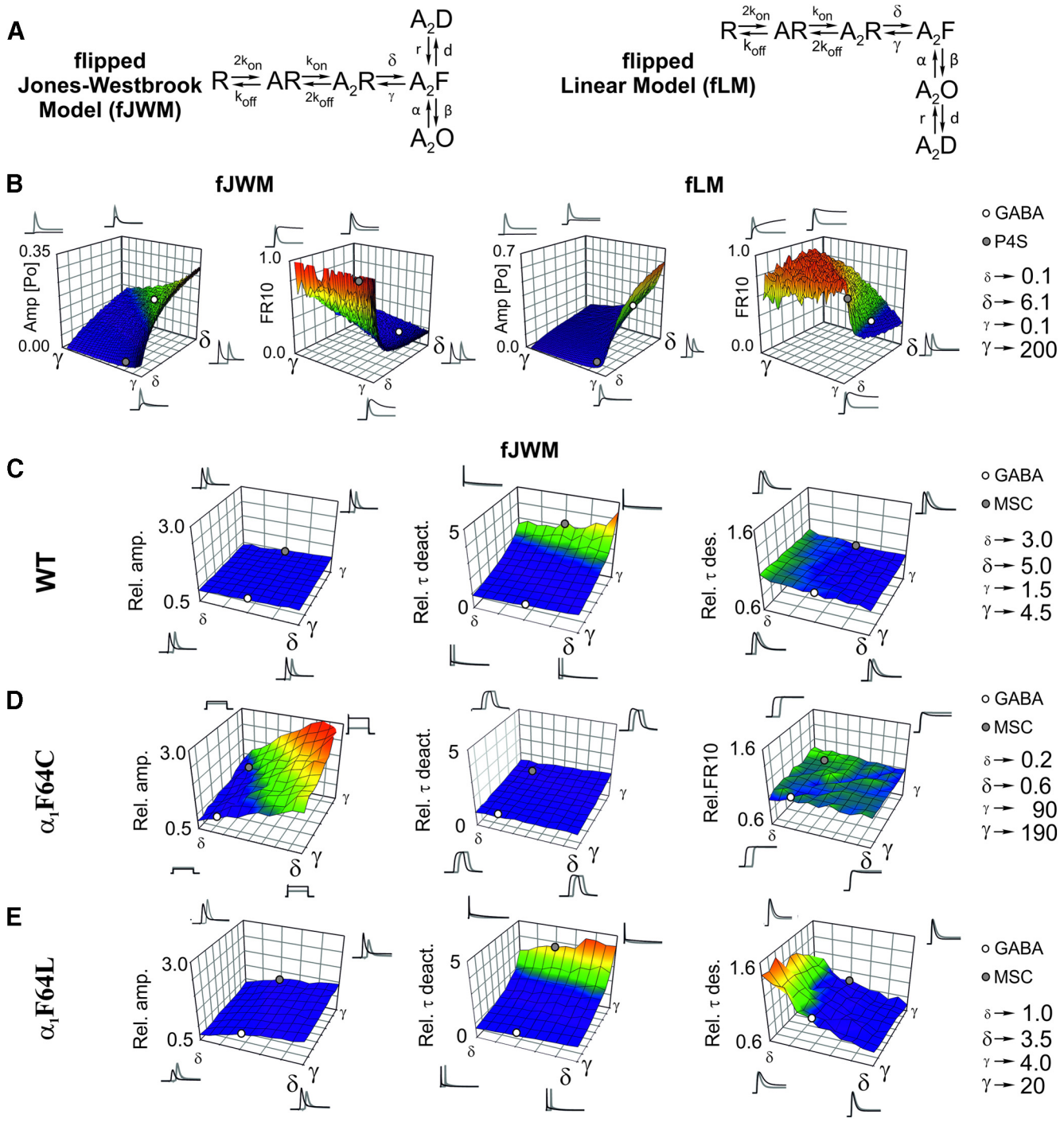

Figure 10. Model simulations based on the JWM and the LM, including the flipped (preactivated) state. ***A***, Kinetic schemes from Figure 9 with an additional single flipped (preactivated) state. Left, fJWM. Right, fLM. ***B***, Surface plots that depict the dependence of amplitude and FR(10) on flipping rate constants for fJWM (left) and fLM (right). The white dot indicates the flipping transition rate constants determined for GABA application in wild-type receptors (see Table 1 for values). The gray dot indicates flipping transition rate constants determined for P4S application in wild type (WT; Table 2). The insets depict the simulated current time course for the boundary values of the parameters (black line) superimposed on simulated WT GABA currents for comparison (gray line). For the FR(10) plot inset, the currents were normalized to visualize the difference in desensitization. For both schemes, FR(10) was affected by changes in the flip rate constants. Numerical values of the rate constants represented by large and small characters, defining the parameter's range, are given on the right. ***C–E***, Surface plots that depict the possible mechanisms of muscimol's effects on the examined receptors calculated for the fJWM. The *Z*-axes show the values of the kinetic parameters relative to those simulated for GABA application in a given receptor (the white dot depicts a *Z* value of 1; Table 4). The white dot indicates the flipping transition rate constants determined for GABA application. The gray dot indicates the flipping transition rate constants for muscimol application (Table 4). The insets depict the simulated current time courses for the boundary values of the parameters (black line) superimposed on simulated GABA currents for comparison (gray line). For the desensitization and deactivation plot inset, the currents were normalized to visualize differences. Numerical values of the rate constants represented by large and small characters are given on the right. In ***B–E***, all of the axis scales are linear, and horizontal scales are the same across panels, defined by small and large characters on the right. For presentation purposes in surface plots presented in ***C–E***, γ and δ axes were changed with respect to those in ***B***. *Z*-axis scaling is identical in columns across ***C–E***. The time scales of the insets differ to best visualize variations of the kinetic parameter presented on a given surface plot. Due to stochastic nature of Monte Carlo simulations, surface plots show some degree of roughness (see Materials and Methods). Kinetic rate constants are given in ms $^{-1}$.

segments (Im et al., 1996; Dalziel et al., 2000; Chang et al., 2003; Fisher, 2004; Gonzales et al., 2008) or proposed an interaction between N-terminal and transmembrane segments (Bianchi and Macdonald, 2001). Moreover, the application of voltage-clamp fluorometry provided evidence that desensitization is not associated with alterations in the vicinity of ligand binding pocket residues (Muroi et al., 2006; Akk et al., 2011; Keramidas and Lynch, 2013). These findings suggest that α_1F64 is not a key structural determinant of microscopic desensitization, although its mutation might affect other transitions that could affect macroscopic desensitization because of so-called functional coupling of the receptor's conformational transitions (Colquhoun, 1998; Mozrzymas et al., 2003a). In our experiments, currents elicited by a saturating concentration of the partial agonist P4S did not show rapid desensitization in wild-type receptors seemingly supporting this possibility. Moreover, the partial rescue of macroscopic desensitization for α_1F64L mutants when muscimol was used further suggests that desensitization is not structurally disrupted but rather appears to be masked by other changes in receptor gating. This scenario is exemplified by the observation of Bianchi and Macdonald (2003), who found that "nondesensitizing" δ subunit-containing $GABA_ARs$ can be turned to desensitizing subunit-containing $GABA_ARs$ by applying the efficacy-enhancing modulator tetrahydrodeoxycorticosterone, whereas desensitizing γ_2 subunit-containing $GABA_ARs$ become "nondesensitizing" for a partial agonist, similar to our observations.

To reveal the conformational transitions affected by the α_1F64 mutation, model simulations were used. Surprisingly, the JWM properly reproduced wild-type $GABA_AR$ behavior, but it failed to describe our observations for α_1F64C mutants. A considerably better reproduction of our data, especially for mutants, was obtained with the LM, which was previously reported to be problematic, at least for wild-type receptors (Bianchi et al., 2007, their discussion). Our analysis indicates that the major reason for the failure of the JWM is the lack of flipping transitions that appear to be affected by the considered mutations. Indeed, the inclusion of just one flipping state in this model allowed us to properly reproduce all of our major findings. The models proposed for GlyRs and AChRs (Burzomato et al., 2004; Lape et al., 2008) postulate flipped states also for partially liganded states, and their number is still kept relatively low by assuming concerted transitions (Lape et al., 2008; Colquhoun and Lape, 2012). More recently, however, Mukhtasimova et al. (2009) proposed that each subunit could flip independently, yielding a fit improvement but also substantially increasing the number of free parameters. To allow for docking an agonist at the binding site and subsequent activation, Jadey and Auerbach (2012) suggested that receptors may visit several short-lived conformational states when traversing the energy barrier between closed and open conformations. These states, however, are nonconducting and cannot be distinguished based on macroscopic current analysis. We concede that the reliable estimation of increased number of rate constants was not feasible, and the minimum requirement models were considered.

Fitting of our data using the fJWM and fLM did not allow us to unequivocally discriminate between these schemes. Importantly, for the fJWM, a good reproduction of all of the major observations for wild-type and mutant receptors activated by GABA, P4S, and muscimol could be obtained by mainly manipulating the flipping rate constants. Changes in desensitization rates had a minor impact on the overall fit quality. In the case of the fLM, opening/closing rates had to be changed, and this modification was indispensable for reproducing experimental observations. Considering that α_1F64 is localized at the binding site, close to where flipping is suspected to occur (Colquhoun and Lape, 2012) or at least initiated (Jadey and Auerbach, 2012), the predictions of the fJWM appear more plausible. Indeed, the structural determinants of the channel's postflipping gating transitions are believed to be distant from the binding sites (Cederholm et al., 2009; Miller and Smart, 2010) and likely less sensitive to the α_1F64 mutation. Interestingly, the model proposed by Keramidas and Harrison (2010, their Scheme 1) for rate constants determined for $\alpha_1\beta_1\gamma_2$ receptors (low occupancy of A_2R^*) bears a resemblance to the fJWM considered here, but some features of our fLM are also embedded. It is possible that fitting of our data with more complex schemes (more closed, open, and desensitized states) would require a model that comprises elements of both the fJWM and fLM. Other schemes proposed based on the log-likelihood fitting of single-channel data also postulate a nonconducting gateway, regardless of specific gating connectivity (Lema and Auerbach, 2006).

Our results indicate that α_1F64 mutations affect both binding and flipping (i.e., gating), but the molecular mechanisms of such a dual effect remain unknown. Several aromatic amino acids exhibit cation-π interactions with GABA, but the α_1F64 residue does not, and it was suggested to solely contribute to the region's hydrophobicity (Padgett et al., 2007). However, in recent molecular dynamics simulations, Carpenter et al. (2012) have showed that α_1F64 is one of the residues that contacts GABA most often, suggesting a more direct interaction with the agonist. Intriguingly, mutations of other aromatic residues at the agonist binding site (e.g., β_2Y97, β_2Y157, β_2Y205) mainly affected binding properties, although some effects on gating have been suggested (Laha and Tran, 2013). Numerous other residues in the proximity of the binding site located on different loops were shown to influence gating in various types of $GABA_ARs$: loop A, β_2L99C (Boileau et al., 2002); loop B, β_2E155C (Newell et al., 2004); loop C, β_2E153 (Venkatachalan and Czajkowski, 2008). Salt bridge-forming residues β_2D163 (loop B) and α_1R120 (loop E) were also found to affect gating (Laha and Wagner, 2011). Thus, receptor gating may be sensitive to mutations at different locations at the binding site, suggesting that transfer of binding energy to gating may rely on structurally complex mechanisms. Consistent with the notion that flipping is expected to occur close to binding sites (Colquhoun and Lape, 2012), our results prompted us to hypothesize that alterations in gating that result from mutations at the binding site might partially reflect modifications of flipping states. Our results indicate that α_1F64 is involved in flipping, but the role of other binding site residues requires further studies. Indeed, the conformational changes involved in "flipping" may correspond to one or several of the steps in the "Brownian conformational wave" postulated by Auerbach and colleagues (Auerbach, 2005; Jadey and Auerbach, 2012).

An extensive and so far weakly explored field is the role of flipping in the modulation of $GABA_ARs$ by a large repertoire of physiologically and clinically relevant agents. Introduction of the concept of flipping states led to a redefinition of partial agonism (Lape et al., 2008). In a more recent study, Gielen et al. (2012) proposed that the actions of benzodiazepines can be explained by the modulation of flipping transitions. The consideration of flipping states may shed new light on the mechanisms of action of many other important $GABA_AR$ modulators.

In conclusion, we provide evidence that the α_1F64 residue is important for both the binding and gating properties of $GABA_ARs$. Although mutation of the α_1F64 residue resulted in a multiplicity of kinetic manifestations, our data indicate that the

modification of flipping transitions represents an important mechanism underlying alterations of receptor gating.

References

Absalom N, Eghorn LF, Villumsen IS, Karim N, Bay T, Olsen JV, Knudsen GM, Bräuner-Osborne H, Frølund B, Clausen RP, Chebib M, Wellendorph P (2012) $\alpha4\beta\delta$ GABA(A) receptors are high-affinity targets for γ-hydroxybutyric acid (GHB). Proc Natl Acad Sci U S A 109:13404–13409. CrossRef Medline

Akk G (2002) Contributions of the non-alpha subunit residues (loop D) to agonist binding and channel gating in the muscle nicotinic acetylcholine receptor. J Physiol 544(Pt 3):695–705. Medline

Akk G, Li P, Bracamontes J, Wang M, Steinbach JH (2011) Pharmacology of structural changes at the GABA(A) receptor transmitter binding site. Br J Pharmacol 162:840–850. CrossRef Medline

Amin J, Weiss DS (1993) GABAA receptor needs two homologous domains of the beta-subunit for activation by GABA but not by pentobarbital. Nature 366:565–569. CrossRef Medline

Auerbach A (2005) Gating of acetylcholine receptor channels: Brownian motion across a broad transition state. Proc Natl Acad Sci U S A 102:1408–1412. CrossRef Medline

Bafna PA, Jha A, Auerbach A (2009) Aromatic residues εTrp-55 and ΔTrp-57 and the activation of acetylcholine receptor channels. J Biol Chem 284:8582–8588. Medline

Bianchi MT, Macdonald RL (2001) Mutation of the 9′ leucine in the GABA(A) receptor gamma2L subunit produces an apparent decrease in desensitization by stabilizing open states without altering desensitized states. Neuropharmacology 41:737–744. CrossRef Medline

Bianchi MT, Macdonald RL (2003) Neurosteroids shift partial agonist activation of $GABA_A$ receptor channels from low- to high-efficacy gating patterns. J Neurosci 23:10934–10943. Medline

Bianchi MT, Botzolakis EJ, Haas KF, Fisher JL, Macdonald RL (2007) Microscopic kinetic determinants of macroscopic currents: insights from coupling and uncoupling of GABAA receptor desensitization and deactivation. J Physiol 584:769–787. CrossRef Medline

Boileau AJ, Newell JG, Czajkowski C (2002) GABA(A) receptor beta 2 Tyr97 and Leu99 line the GABA-binding site. Insights into mechanisms of agonist and antagonist actions. J Biol Chem 277:2931–2937. CrossRef Medline

Bouzat C (2012) New insights into the structural bases of activation of Cys-loop receptors. J Physiol Paris 106:23–33. CrossRef Medline

Burzomato V, Beato M, Groot-Kormelink PJ, Colquhoun D, Sivilotti LG (2004) Single-channel behavior of heteromeric $\alpha1\beta$ glycine receptors: an attempt to detect a conformational change before the channel opens. J Neurosci 24:10924–10940. CrossRef Medline

Carpenter TS, Lau EY, Lightstone FC (2012) A role for loop F in modulating GABA binding affinity in the GABA(A) receptor. J Mol Biol 422:310–323. CrossRef Medline

Cederholm JM, Schofield PR, Lewis TM (2009) Gating mechanisms in Cys-loop receptors. Eur Biophys J 39:37–49. CrossRef Medline

Chang CS, Olcese R, Olsen RW (2003) A single M1 residue in the beta2 subunit alters channel gating of GABAA receptor in anesthetic modulation and direct activation. J Biol Chem 278:42821–42828. CrossRef Medline

Chen C, Okayama H (1987) High-efficiency transformation of mammalian cells by plasmid DNA. Mol Cell Biol 7:2745–2752. Medline

Colquhoun D (1998) Binding, gating, affinity and efficacy: the interpretation of structure-activity relationships for agonists and of the effects of mutating receptors. Br J Pharmacol 125:924–947. Medline

Colquhoun D, Hawkes AG (1982) On the stochastic properties of bursts of single ion channel openings and of clusters of bursts. Philos Trans R Soc Lond B Biol Sci 300:1–59. CrossRef Medline

Colquhoun D, Hawkes AG (1995) Desensitization of N-methyl-D-aspartate receptors: a problem of interpretation. Proc Natl Acad Sci U S A 92:10327–10329. CrossRef Medline

Colquhoun D, Lape R (2012) Perspectives on: conformational coupling in ion channels: allosteric coupling in ligand-gated ion channels. J Gen Physiol 140:599–612. CrossRef Medline

Cromer BA, Morton CJ, Parker MW (2002) Anxiety over GABA(A) receptor structure relieved by AChBP. Trends Biochem Sci 27:280–287. CrossRef Medline

Dalziel JE, Cox GB, Gage PW, Birnir B (2000) Mutating the highly conserved second membrane-spanning region 9′ leucine residue in the alpha(1) or beta(1) subunit produces subunit-specific changes in the function of human alpha(1)beta(1) gamma-aminobutyric acid(A) receptors. Mol Pharmacol 57:875–882. Medline

De Koninck Y, Mody I (1994) Noise analysis of miniature IPSCs in adult rat brain slices: properties and modulation of synaptic GABAA receptor channels. J Neurophysiol 71:1318–1335. Medline

Drafts BC, Fisher JL (2006) Identification of structures within GABAA receptor alpha subunits that regulate the agonist action of pentobarbital. J Pharmacol Exp Ther 318:1094–1101. CrossRef Medline

Feng HJ, Bianchi MT, Macdonald RL (2004) Pentobarbital differentially modulates $\alpha1\beta3\delta$ and $\alpha1\beta3\gamma2$L GABAA receptor currents. Mol Pharmacol 66:988–1003. CrossRef Medline

Fisher JL (2004) A mutation in the GABAA receptor alpha 1 subunit linked to human epilepsy affects channel gating properties. Neuropharmacology 46:629–637. CrossRef Medline

Gay EA, Giniatullin R, Skorinkin A, Yakel JL (2008) Aromatic residues at position 55 of rat alpha7 nicotinic acetylcholine receptors are critical for maintaining rapid desensitization. J Physiol 586:1105–1115. Medline

Ghavanini AA, Isbasescu IM, Mathers DA, Puil E (2006) Optimizing fluctuation analysis of GABAAergic IPSCs for accurate unitary currents. J Neurosci Methods 158:150–156. CrossRef Medline

Gielen MC, Lumb MJ, Smart TG (2012) Benzodiazepines modulate $GABA_A$ receptors by regulating the preactivation step after GABA binding. J Neurosci 32:5707–5715. CrossRef Medline

Gingrich KJ, Burkat PM, Roberts WA (2009) Pentobarbital produces activation and block of $\alpha1\beta2\gamma2$S GABAA receptors in rapidly perfused whole cells and membrane patches: divergent results can be explained by pharmacokinetics. J Gen Physiol 133:171–188. CrossRef Medline

Goldschen-Ohm MP, Wagner DA, Jones MV (2011) Three arginines in the GABAA receptor binding pocket have distinct roles in formation and stability of agonist- versus antagonist-bound complexes. Mol Pharmacol 80:647–656. CrossRef Medline

Gonzales EB, Bell-Horner CL, Dibas MI, Huang RQ, Dillon GH (2008) Stoichiometric analysis of the TM2 6′ phenylalanine mutation on desensitization in alpha1beta2 and alpha1beta2gamma2 GABA A receptors. Neurosci Lett 431:184–189. CrossRef Medline

Holden JH, Czajkowski C (2002) Different residues in the GABA(A) receptor alpha 1T60-alpha 1K70 region mediate GABA and SR-95531 actions. J Biol Chem 277:18785–18792. CrossRef Medline

Im HK, Im WB, Von Voigtlander PF, Carter DB, Murray BH, Jacobsen EJ (1996) Characterization of U-101017 as a GABA(A) receptor ligand of dual functionality. Brain Res 714:165–168. CrossRef Medline

Jadey S, Auerbach A (2012) An integrated catch-and-hold mechanism activates nicotinic acetylcholine receptors. J Gen Physiol 140:17–28. CrossRef Medline

Jonas P (1995) Fast application of agonists to isolated membrane patches. In: Single-channel recording (Sakmann B, Neher E, eds), pp 231–243. New York: Plenum.

Jones MV, Westbrook GL (1995) Desensitized states prolong GABAA channel responses to brief agonist pulses. Neuron 15:181–191. CrossRef Medline

Jones MV, Sahara Y, Dzubay JA, Westbrook GL (1998) Defining affinity with the $GABA_A$ receptor. J Neurosci 18:8590–8604. Medline

Jones MV, Jonas P, Sahara Y, Westbrook GL (2001) Microscopic kinetics and energetics distinguish gabaa receptor agonists from antagonists. Biophys J 81:2660–2670. CrossRef Medline

Karlsson U, Druzin M, Johansson S (2011) Cl(−) concentration changes and desensitization of GABA(A) and glycine receptors. J Gen Physiol 138:609–626. CrossRef Medline

Kash TL, Jenkins A, Kelley JC, Trudell JR, Harrison NL (2003) Coupling of agonist binding to channel gating in the GABA(A) receptor. Nature 421:272–275. CrossRef Medline

Keramidas A, Harrison NL (2010) The activation mechanism of alpha1beta2gamma2S and alpha3beta3gamma2S GABAA receptors. J Gen Physiol 135:59–75. CrossRef Medline

Keramidas A, Lynch JW (2013) An outline of desensitization in pentameric ligand-gated ion channel receptors. Cell Mol Life Sci 70:1241–1253. CrossRef Medline

Laha KT, Tran PN (2013) Multiple tyrosine residues at the GABA binding pocket influence surface expression and mediate kinetics of the GABAA receptor. J Neurochem 124:200–209. CrossRef Medline

Laha KT, Wagner DA (2011) A state-dependent salt-bridge interaction ex-

ists across the beta/alpha intersubunit interface of the GABAA receptor. Mol Pharmacol 79:662–671. CrossRef Medline

Lape R, Colquhoun D, Sivilotti LG (2008) On the nature of partial agonism in the nicotinic receptor superfamily. Nature 454:722–727. Medline

Lape R, Plested AJ, Moroni M, Colquhoun D, Sivilotti LG (2012) The α1K276E startle disease mutation reveals multiple intermediate states in the gating of glycine receptors. J Neurosci 32:1336–1352. CrossRef Medline

Lema GM, Auerbach A (2006) Modes and models of GABA(A) receptor gating. J Physiol 572(Pt 1):183–200. Medline

Maconochie DJ, Zempel JM, Steinbach JH (1994) How quickly can GABAA receptors open? Neuron 12:61–71. CrossRef Medline

Mercado J, Czajkowski C (2008) Gamma-aminobutyric acid (GABA) and pentobarbital induce different conformational rearrangements in the GABA A receptor alpha1 and beta2 pre-M1 regions. J Biol Chem 283: 15250–15257. CrossRef Medline

Miller PS, Smart TG (2010) Binding, activation and modulation of Cys-loop receptors. Trends Pharmacol Sci 31:161–174. CrossRef Medline

Moroni M, Biro I, Giugliano M, Vijayan R, Biggin PC, Beato M, Sivilotti LG (2011) Chloride ions in the pore of glycine and GABA channels shape the time course and voltage dependence of agonist currents. J Neurosci 31: 14095–14106. CrossRef Medline

Mortensen M, Kristiansen U, Ebert B, Frølund B, Krogsgaard-Larsen P, Smart TG (2004) Activation of single heteromeric GABA(A) receptor ion channels by full and partial agonists. J Physiol 557:389–413. CrossRef Medline

Mortensen M, Ebert B, Wafford K, Smart TG (2010) Distinct activities of GABA agonists at synaptic- and extrasynaptic-type GABAA receptors. J Physiol 588(Pt 8):1251–1268. CrossRef Medline

Mozrzymas JW, Barberis A, Michalak K, Cherubini E (1999) Chlorpromazine inhibits miniature GABAergic currents by reducing the binding and by increasing the unbinding rate of GABA$_A$ receptors. J Neurosci 19: 2474–2488. Medline

Mozrzymas JW, Barberis A, Mercik K, Zarnowska ED (2003a) Binding sites, singly bound states, and conformation coupling shape GABA-evoked currents. J Neurophysiol 89:871–883. Medline

Mozrzymas JW, Zarnowska ED, Pytel M, Mercik K (2003b) Modulation of GABA$_A$ receptors by hydrogen ions reveals synaptic GABA transient and a crucial role of the desensitization process. J Neurosci 23:7981–7992. Medline

Mukhtasimova N, Lee WY, Wang HL, Sine SM (2009) Detection and trapping of intermediate states priming nicotinic receptor channel opening. Nature 459:451–454. CrossRef Medline

Muroi Y, Czajkowski C, Jackson MB (2006) Local and global ligand-induced changes in the structure of the GABA(A) receptor. Biochemistry 45:7013–7022. CrossRef Medline

Newell JG, McDevitt RA, Czajkowski C (2004) Mutation of glutamate 155 of the GABA$_A$ receptor β2 subunit produces a spontaneously open channel: a trigger for channel activation. J Neurosci 24:11226–11235. CrossRef Medline

Padgett CL, Hanek AP, Lester HA, Dougherty DA, Lummis SC (2007) Unnatural amino acid mutagenesis of the GABA(A) receptor binding site residues reveals a novel cation-π interaction between GABA and β_2 Tyr97. J Neurosci 27:886–892. CrossRef Medline

Petrini EM, Nieus T, Ravasenga T, Succol F, Guazzi S, Benfenati F, Barberis A (2011) Influence of GABA$_A$R monoliganded states on GABAergic responses. J Neurosci 31:1752–1761. CrossRef Medline

Scheller M, Forman SA (2002) Coupled and uncoupled gating and desensitization effects by pore domain mutations in GABA$_A$ receptors. J Neurosci 22:8411–8421. Medline

Sigel E, Baur R, Kellenberger S, Malherbe P (1992) Point mutations affecting antagonist affinity and agonist dependent gating of GABAA receptor channels. EMBO J 11:2017–2023. Medline

Sigworth FJ (1980) The variance of sodium current fluctuations at the node of Ranvier. J Physiol 307:97–129. Medline

Smith GB, Olsen RW (1995) Functional domains of GABAA receptors. Trends Pharmacol Sci 16:162–168. CrossRef Medline

Spier AD, Lummis SC (2000) The role of tryptophan residues in the 5-hydroxytryptamine(3) receptor ligand binding domain. J Biol Chem 275:5620–5625. CrossRef Medline

Torres VI, Weiss DS (2002) Identification of a tyrosine in the agonist binding site of the homomeric rho1 gamma-aminobutyric acid (GABA) receptor that, when mutated, produces spontaneous opening. J Biol Chem 277:43741–43748. CrossRef Medline

Tran PN, Laha KT, Wagner DA (2011) A tight coupling between beta(2)Y97 and beta(2)F200 of the GABA(A) receptor mediates GABA binding. J Neurochem 119:283–293. CrossRef Medline

Twyman RE, Rogers CJ, Macdonald RL (1989) Differential regulation of gamma-aminobutyric acid receptor channels by diazepam and phenobarbital. Ann Neurol 25:213–220. CrossRef Medline

Ueno S, Bracamontes J, Zorumski C, Weiss DS, Steinbach JH (1997) Bicuculline and gabazine are allosteric inhibitors of channel opening of the GABA$_A$ receptor. J Neurosci 17:625–634. Medline

Venkatachalan SP, Czajkowski C (2008) A conserved salt bridge critical for GABA(A) receptor function and loop C dynamics. Proc Natl Acad Sci U S A 105:13604–13609. CrossRef Medline

Wagner DA, Czajkowski C, Jones MV (2004) An arginine involved in GABA binding and unbinding but not gating of the GABA$_A$ receptor. J Neurosci 24:2733–2741. CrossRef Medline

Xie Y, Cohen JB (2001) Contributions of Torpedo nicotinic acetylcholine receptor gamma Trp-55 and delta Trp-57 to agonist and competitive antagonist function. J Biol Chem 276:2417–2426. CrossRef Medline

Xiu X, Hanek AP, Wang J, Lester HA, Dougherty DA (2005) A unified view of the role of electrostatic interactions in modulating the gating of Cys loop receptors. J Biol Chem 280:41655–41666. CrossRef Medline